8 MIMO II: capacity and multiplexing architectures

In this chapter, we will look at the capacity of MIMO fading channels and discuss transceiver architectures that extract the promised multiplexing gains from the channel. We particularly focus on the scenario when the transmitter does not know the channel realization. In the fast fading MIMO channel, we show the following:

- At high SNR, the capacity of the i.i.d. Rayleigh fast fading channel scales like $n_{\min} \log \mathsf{SNR}$ bits/s/Hz, where $n_{\min}$ is the minimum of the number of transmit antennas n_{t} and the number of receive antennas n_{r}. This is a degree-of-freedom gain.
- At low SNR, the capacity is approximately $n_{\mathrm{r}} \mathsf{SNR} \log_2 e$ bits/s/Hz. This is a receive beamforming power gain.
- At all SNR, the capacity scales linearly with $n_{\min}$. This is due to a combination of a power gain and a degree-of-freedom gain.

Furthermore, there is a transmit beamforming gain together with an opportunistic communication gain if the transmitter can track the channel as well.

Over a deterministic time-invariant MIMO channel, the capacity-achieving transceiver architecture is simple (cf. Section 7.1.1): independent data streams are multiplexed in an appropriate coordinate system (cf. Figure 7.2). The receiver transforms the received vector into another appropriate coordinate system to separately decode the different data streams. Without knowledge of the channel at the transmitter the choice of the coordinate system in which the independent data streams are multiplexed has to be fixed a priori. In conjunction with joint decoding, we will see that this transmitter architecture achieves the capacity of the fast fading channel. This architecture is also called V-BLAST[1] in the literature.

---

[1] Vertical Bell Labs Space-Time Architecture. There are several versions of V-BLAST with different receiver structures but they all share the same transmitting architecture of multiplexing independent streams, and we take this as its defining feature.

In Section 8.3, we discuss receiver architectures that are simpler than joint ML decoding of the independent streams. While there are several receiver architectures that can support the full degrees of freedom of the channel, a particular architecture, the MMSE-SIC, which uses a combination of minimum mean square estimation (MMSE) and successive interference cancellation (SIC), achieves capacity.

The performance of the slow fading MIMO channel is characterized through the outage probability and the corresponding outage capacity. At low SNR, the outage capacity can be achieved, to a first order, by using one transmit antenna at a time, achieving a full diversity gain of n_t n_r and a power gain of n_r. The outage capacity at high SNR, on the other hand, benefits from a degree-of-freedom gain as well; this is more difficult to characterize succinctly and its analysis is relegated until Chapter 9.

Although it achieves the capacity of the *fast fading* channel, the V-BLAST architecture is strictly suboptimal for the *slow fading* channel. In fact, it does not even achieve the full diversity gain promised by the MIMO channel. To see this, consider transmitting independent data streams directly over the transmit antennas. In this case, the diversity of each data stream is limited to just the receive diversity. To extract the full diversity from the channel, one needs to code *across* the transmit antennas. A modified architecture, D-BLAST[2], which combines transmit antenna coding with MMSE-SIC, not only extracts the full diversity from the channel but its performance also comes close to the outage capacity.

8.1 The V-BLAST architecture

We start with the time-invariant channel (cf. (7.1))

$$\mathbf{y}[m] = \mathbf{H}\mathbf{x}[m] + \mathbf{w}[m], \qquad m = 1, 2, \ldots \qquad (8.1)$$

When the channel matrix $\mathbf{H}$ is known to the transmitter, we have seen in Section 7.1.1 that the optimal strategy is to transmit independent streams in the directions of the eigenvectors of $\mathbf{H}^*\mathbf{H}$, i.e., in the coordinate system defined by the matrix $\mathbf{V}$, where $\mathbf{H} = \mathbf{U}\mathbf{\Lambda}\mathbf{V}^*$ is the singular value decomposition of $\mathbf{H}$. This coordinate system is channel-dependent. With an eye towards dealing with the case of fading channels where the channel matrix is *unknown* to the transmitter, we generalize this to the architecture in Figure 8.1, where the independent data streams, n_t of them, are multiplexed in some arbitrary

---

[2] Diagonal Bell Labs Space-Time Architecture

Figure 8.1 The V-BLAST architecture for communicating over the MIMO channel.
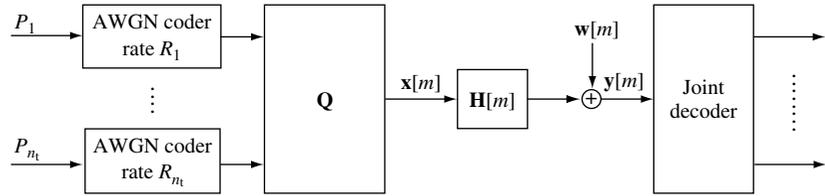
coordinate system given by a unitary matrix $\mathbf{Q}$, not necessarily dependent on the channel matrix $\mathbf{H}$. This is the V-BLAST architecture. The data streams are decoded jointly. The kth data stream is allocated a power P_k (such that the sum of the powers, $P_1 + \cdots + P_{n_t}$, is equal to P, the total transmit power constraint) and is encoded using a capacity-achieving Gaussian code with rate R_k. The total rate is $R = \sum_{k=1}^{n_t} R_k$.

As special cases:

- If $\mathbf{Q} = \mathbf{V}$ and the powers are given by the waterfilling allocations, then we have the capacity-achieving architecture in Figure 7.2.
- If $\mathbf{Q} = \mathbf{I}_{n_t}$, then independent data streams are sent on the different transmit antennas.

Using a sphere-packing argument analogous to the ones used in Chapter 5, we will argue an upper bound on the highest reliable rate of communication:

$$R < \log \det \left(\mathbf{I}_{n_r} + \frac{1}{N_0} \mathbf{H} \mathbf{K}_x \mathbf{H}^* \right) \text{bits/s/Hz}. \tag{8.2}$$

Here $\mathbf{K}_x$ is the covariance matrix of the transmitted signal $\mathbf{x}$ and is a function of the multiplexing coordinate system and the power allocations:

$$\mathbf{K}_x := \mathbf{Q} \, \text{diag}\{P_1, \ldots, P_{n_t}\} \mathbf{Q}^*. \tag{8.3}$$

Considering communication over a block of time symbols of length N, the received vector, of length $n_r N$, lies with high probability in an ellipsoid of volume proportional to

$$\det(N_0 \mathbf{I}_{n_r} + \mathbf{H} \mathbf{K}_x \mathbf{H}^*)^N. \tag{8.4}$$

This formula is a direct generalization of the corresponding volume formula (5.50) for the parallel channel, and is justified in Exercise 8.2. Since we have to allow for non-overlapping noise spheres (of radius $\sqrt{N_0}$ and, hence, volume proportional to $N_0^{n_r N}$) around each codeword to ensure reliable

communication, the maximum number of codewords that can be packed is the ratio

$$\frac{\det(N_0\mathbf{I}_{n_r} + \mathbf{H}\mathbf{K}_x\mathbf{H}^*)^N}{N_0^{n_r N}}. \tag{8.5}$$

We can now conclude the upper bound on the rate of reliable communication in (8.2).

Is this upper bound actually achievable by the V-BLAST architecture? Observe that *independent* data streams are multiplexed in V-BLAST; perhaps coding across the streams is required to achieve the upper bound (8.2)? To get some insight on this question, consider the special case of a MISO channel ($n_r = 1$) and set $\mathbf{Q} = \mathbf{I}_{n_t}$ in the architecture, i.e., independent streams on each of the transmit antennas. This is precisely an uplink channel, as considered in Section 6.1, drawing an analogy between the transmit antennas and the users. We know from the development there that the sum capacity of this uplink channel is

$$\log\left(1 + \frac{\sum_{k=1}^{n_t} |h_k|^2 P_k}{N_0}\right). \tag{8.6}$$

This is precisely the upper bound (8.2) in this special case. Thus, the V-BLAST architecture, with independent data streams, is sufficient to achieve the upper bound (8.2). In the general case, an analogy can be drawn between the V-BLAST architecture and an uplink channel with n_r receive antennas and channel matrix $\mathbf{HQ}$; just as in the single receive antenna case, the upper bound (8.2) is the sum capacity of this uplink channel and therefore achievable using the V-BLAST architecture. This uplink channel is considered in greater detail in Chapter 10 and its information theoretic analysis is in Appendix B.9.

8.2 Fast fading MIMO channel

The fast fading MIMO channel is

$$\mathbf{y}[m] = \mathbf{H}[m]\mathbf{x}[m] + \mathbf{w}[m], \qquad m = 1, 2, \ldots, \tag{8.7}$$

where $\{\mathbf{H}[m]\}$ is a random fading process. To properly define a notion of capacity (achieved by averaging of the channel fading over time), we make the technical assumption (as in the earlier chapters) that $\{\mathbf{H}[m]\}$ is a stationary and ergodic process. As a normalization, let us suppose that $\mathbb{E}[|h_{ij}|^2] = 1$. As in our earlier study, we consider coherent communication: the receiver tracks the channel fading process exactly. We first start with the situation when the transmitter has only a statistical characterization of the fading channel. Finally, we look at the case when the transmitter also perfectly tracks the fading

channel (full CSI); this situation is very similar to that of the time-invariant MIMO channel.

8.2.1 Capacity with CSI at receiver

Consider using the V-BLAST architecture (Figure 8.1) with a channel-independent multiplexing coordinate system $\mathbf{Q}$ and power allocations $P_1, \ldots, P_{n_t}$. The covariance matrix of the transmit signal is $\mathbf{K}_x$ and is not dependent on the channel realization. The rate achieved in a given channel state $\mathbf{H}$ is

$$\log \det \left(\mathbf{I}_{n_r} + \frac{1}{N_0} \mathbf{H} \mathbf{K}_x \mathbf{H}^* \right).$$ (8.8)

As usual, by coding over many coherence time intervals of the channel, a long-term rate of reliable communication equal to

$$\mathbb{E}_{\mathbf{H}} \left[\log \det \left(\mathbf{I}_{n_r} + \frac{1}{N_0} \mathbf{H} \mathbf{K}_x \mathbf{H}^* \right) \right]$$ (8.9)

is achieved. We can now choose the covariance $\mathbf{K}_x$ as a function of the channel *statistics* to achieve a reliable communication rate of

$$C = \max_{\mathbf{K}_x : \operatorname{Tr}[\mathbf{K}_x] \leq P} \mathbb{E} \left[\log \det \left(\mathbf{I}_{n_r} + \frac{1}{N_0} \mathbf{H} \mathbf{K}_x \mathbf{H}^* \right) \right].$$ (8.10)

Here the trace constraint corresponds to the total transmit power constraint. This is indeed the capacity of the fast fading MIMO channel (a formal justification is in Appendix B.7.2). We emphasize that the input covariance is chosen to match the channel statistics rather than the channel realization, since the latter is not known at the transmitter.

The optimal $\mathbf{K}_x$ in (8.10) obviously depends on the stationary distribution of the channel process $\{\mathbf{H}[m]\}$. For example, if there are only a few dominant paths (no more than one in each of the angular bins) that are not time-varying, then we can view $\mathbf{H}$ as being deterministic. In this case, we know from Section 7.1.1 that the optimal coordinate system to multiplex the data streams is in the eigen-directions of $\mathbf{H}^*\mathbf{H}$ and, further, to allocate powers in a waterfilling manner across the eigenmodes of $\mathbf{H}$.

Let us now consider the other extreme: there are many paths (of approximately equal energy) in each of the angular bins. Some insight can be obtained by looking at the angular representation (cf. (7.80)): $\mathbf{H}^a := \mathbf{U}_r^* \mathbf{H} \mathbf{U}_t$. The key advantage of this viewpoint is in statistical modeling: the entries of $\mathbf{H}^a$ are generated by different physical paths and can be modeled as being statistically independent (cf. Section 7.3.5). Here we are interested in the case when the entries of $\mathbf{H}^a$ have zero mean (no single dominant path in any of the angular

windows). Due to independence, it seems reasonable to separately send information in each of the transmit angular windows, with powers corresponding to the strength of the paths in the angular windows. That is, the multiplexing is done in the coordinate system given by $\mathbf{U}_t$ (so $\mathbf{Q} = \mathbf{U}_t$ in (8.3)). The covariance matrix now has the form

$$\mathbf{K}_x = \mathbf{U}_t \mathbf{\Lambda} \mathbf{U}_t^*, \tag{8.11}$$

where $\mathbf{\Lambda}$ is a diagonal matrix with non-negative entries, representing the powers transmitted in the angular windows, so that the sum of the entries is equal to P. This is shown formally in Exercise 8.3, where we see that this observation holds even if the entries of $\mathbf{H}^a$ are only uncorrelated.

If there is additional symmetry among the transmit antennas, such as when the elements of $\mathbf{H}^a$ are i.i.d. $\mathcal{CN}(0, 1)$ (the i.i.d. Rayleigh fading model), then one can further show that equal powers are allocated to each transmit angular window (see Exercises 8.4 and 8.6) and thus, in this case, the optimal covariance matrix is simply

$$\mathbf{K}_x = \left(\frac{P}{n_t} \right) \mathbf{I}_{n_t}. \tag{8.12}$$

More generally, the optimal powers (i.e., the diagonal entries of Λ) are chosen to be the solution to the maximization problem (substituting the angular representation $\mathbf{H} = \mathbf{U}_r \mathbf{H}^a \mathbf{U}_t^*$ and (8.11) in (8.10)):

$$C = \max_{\Lambda : \mathrm{Tr}\{\Lambda\} \leq P} \mathbb{E} \left[\log \det \left(\mathbf{I}_{n_r} + \frac{1}{N_0} \mathbf{U}_r \mathbf{H}^a \mathbf{\Lambda} \mathbf{H}^{a*} \mathbf{U}_r^* \right) \right] \tag{8.13}$$

$$= \max_{\Lambda : \mathrm{Tr}[\Lambda] \leq P} \mathbb{E} \left[\log \det \left(\mathbf{I}_{n_r} + \frac{1}{N_0} \mathbf{H}^a \mathbf{\Lambda} \mathbf{H}^{a*} \right) \right]. \tag{8.14}$$

With equal powers (i.e., the optimal $\mathbf{\Lambda}$ is equal to $(P/n_t)\mathbf{I}_{n_t}$), the resulting capacity is

$$\boxed{C = \mathbb{E} \left[\log \det \left(\mathbf{I}_{n_r} + \frac{\mathsf{SNR}}{n_t} \mathbf{H}\mathbf{H}^* \right) \right],} \tag{8.15}$$

where $\mathsf{SNR} := P/N_0$ is the common SNR at each receive antenna.

If $\lambda_1 \geq \lambda_2 \geq \cdots \geq \lambda_{n_{\min}}$ are the (random) ordered singular values of $\mathbf{H}$, then we can rewrite (8.15) as

$$C = \mathbb{E} \left[\sum_{i=1}^{n_{\min}} \log \left(1 + \frac{\mathsf{SNR}}{n_t} \lambda_i^2 \right) \right]$$

$$= \sum_{i=1}^{n_{\min}} \mathbb{E} \left[\log \left(1 + \frac{\mathsf{SNR}}{n_t} \lambda_i^2 \right) \right]. \tag{8.16}$$

Comparing this expression to the waterfilling capacity in (7.10), we see the contrast between the situation when the transmitter knows the channel and when it does not. When the transmitter knows the channel, it can allocate different amounts of power in the different eigenmodes depending on their strengths. When the transmitter does not know the channel but the channel is sufficiently random, the optimal covariance matrix is identity, resulting in equal amounts of power across the eigenmodes.

8.2.2 Performance gains

The capacity, (8.16), of the MIMO fading channel is a function of the distribution of the singular values, λ_i, of the random channel matrix $\mathbf{H}$. By Jensen's inequality, we know that

$$\sum_{i=1}^{n_{\min}} \log\left(1 + \frac{\mathsf{SNR}}{n_{\mathrm{t}}}\lambda_i^2\right) \leq n_{\min} \log\left(1 + \frac{\mathsf{SNR}}{n_{\mathrm{t}}}\left[\frac{1}{n_{\min}}\sum_{i=1}^{n_{\min}}\lambda_i^2\right]\right), \tag{8.17}$$

with equality if and only if the singular values are all equal. Hence, one would expect a high capacity if the channel matrix $\mathbf{H}$ is sufficiently random and statistically well conditioned, with the overall channel gain well distributed across the singular values. In particular, one would expect such a channel to attain the full degrees of freedom at high SNR.

We plot the capacity for the i.i.d. Rayleigh fading model in Figure 8.2 for different numbers of antennas. Indeed, we see that for such a random channel the capacity of a MIMO system can be very large. At moderate to high SNR, the capacity of an n by n channel is about n times the capacity of a 1 by 1 system. The asymptotic slope of capacity versus SNR in dB scale is proportional to n, which means that the capacity scales with SNR like $n \log \mathsf{SNR}$.

High SNR regime

The performance gain can be seen most clearly in the high SNR regime. At high SNR, the capacity for the i.i.d. Rayleigh channel is given by

$$C \approx n_{\min} \log \frac{\mathsf{SNR}}{n_{\mathrm{t}}} + \sum_{i=1}^{n_{\min}} \mathbb{E}[\log \lambda_i^2], \tag{8.18}$$

and

$$\mathbb{E}[\log \lambda_i^2] > -\infty, \tag{8.19}$$

for all i. Hence, the full $n_{\min}$ degrees of freedom is attained. In fact, further analysis reveals that

$$\sum_{i=1}^{n_{\min}} \mathbb{E}[\log \lambda_i^2] = \sum_{i=|n_{\mathrm{t}}-n_{\mathrm{r}}|+1}^{\max\{n_{\mathrm{t}},n_{\mathrm{r}}\}} \mathbb{E}[\log \chi_{2i}^2], \tag{8.20}$$

Figure 8.2 Capacity of an i.i.d. Rayleigh fading channel. Upper: 4 by 4 channel. Lower: 8 by 8 channel.

C (bits /s / Hz)
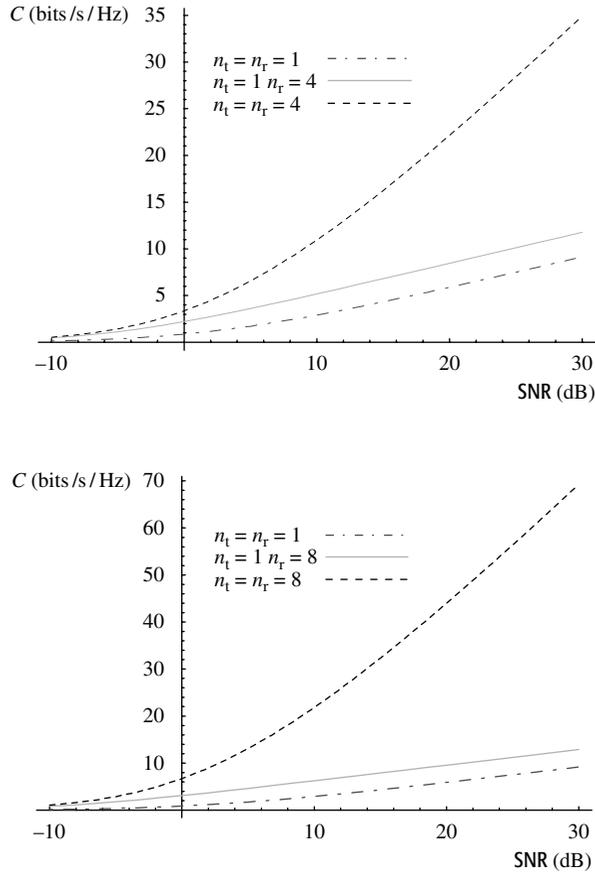
where χ^2_{2i} is a χ-square distributed random variable with $2i$ degrees of freedom.

Note that the number of degrees of freedom is limited by the minimum of the number of transmit and the number of receive antennas, hence, to get a large capacity, we need multiple transmit *and* multiple receive antennas. To emphasize this fact, we also plot the capacity of a 1 by n_r channel in Figure 8.2. This capacity is given by

$$C = \mathbb{E}\left[\log\left(1 + \mathsf{SNR}\sum_{i=1}^{n_r}|h_i|^2\right)\right] \text{ bits/s/Hz.} \tag{8.21}$$

We see that the capacity of such a channel is significantly less than that of an n_r by n_r system in the high SNR range, and this is due to the fact that there is only one degree of freedom in a 1 by n_r channel. The gain in going from a 1 by 1 system to a 1 by n_r system is a *power gain*, resulting in a parallel

shift of the capacity versus SNR curves. At high SNR, a power gain is much less impressive than a degree-of-freedom gain.

Low SNR regime

Here we use the approximation $\log_2(1+x) \approx x\log_2 e$ for x small in (8.15) to get

$$
\begin{aligned}
C &= \sum_{i=1}^{n_{\min}} \mathbb{E}\left[\log\left(1+\frac{\mathsf{SNR}}{n_t}\lambda_i^2\right)\right] \\
&\approx \sum_{i=1}^{n_{\min}} \frac{\mathsf{SNR}}{n_t}\mathbb{E}\left[\lambda_i^2\right]\log_2 e \\
&= \frac{\mathsf{SNR}}{n_t}\mathbb{E}[\mathrm{Tr}[\mathbf{H}\mathbf{H}^*]]\log_2 e \\
&= \frac{\mathsf{SNR}}{n_t}\mathbb{E}\left[\sum_{i,j}|h_{ij}|^2\right]\log_2 e \\
&= n_r\mathsf{SNR}\log_2 e \ \text{bits/s/Hz}.
\end{aligned}
$$

Thus, at low SNR, an n_t by n_r system yields a *power gain* of n_r over a single antenna system. This is due to the fact that the multiple receive antennas can coherently combine their received signals to get a power boost. Note that increasing the number of transmit antennas does not increase the power gain since, unlike the case when the channel is known at the transmitter, *transmit* beamforming cannot be done to constructively add signals from the different antennas. Thus, at low SNR and without channel knowledge at the transmitter, multiple transmit antennas are not very useful: the performance of an n_t by n_r channel is comparable with that of a 1 by n_r channel. This is illustrated in Figure 8.3, which compares the capacity of an n by n channel with that of a 1 by n channel, as a fraction of the capacity of a 1 by 1 channel. We see that at an SNR of about $-20\,\text{dB}$, the capacities of a 1 by 4 channel and a 4 by 4 channel are very similar.

Recall from Chapter 4 that the operating SINR of cellular systems with universal frequency reuse is typically very low. For example, an IS-95 CDMA system may have an SINR per chip of -15 to $-17\,\text{dB}$. The above observation then suggests that just simply overlaying point-to-point MIMO technology on such systems to boost up per link capacity will not provide much additional benefit than just adding antennas at one end. On the other hand, the story is different if the multiple antennas are used to perform multiple access and interference management. This issue will be revisited in Chapter 10.

Another difference between the high and the low SNR regimes is that while channel randomness is crucial in yielding a large capacity gain in the high SNR regime, it plays little role in the low SNR regime. The low SNR result above does not depend on whether the channel gains, $\{h_{ij}\}$, are independent or correlated.

Figure 8.3 Low SNR capacities. Upper: a 1 by 4 and a 4 by 4 channel. Lower: a 1 by 8 an 8 by 8 channel. Capacity is a fraction of the 1 by 1 channel in each case.
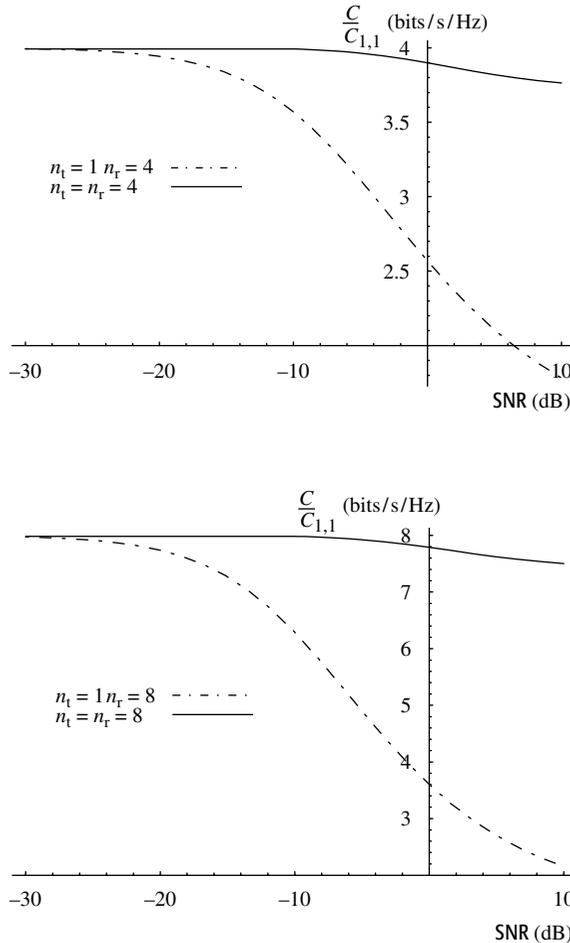
Large antenna array regime

We saw that in the high SNR regime, the capacity increases linearly with the minimum of the number of transmit and the number of receive antennas. This is a degree-of-freedom gain. In the low SNR regime, the capacity increases linearly with the number of receive antennas. This is a power gain. Will the combined effect of the two types of gain yield a linear growth in capacity at *any* SNR, as we scale up both n_t and n_r? Indeed, this turns out to be true. Let us focus on the square channel $n_t = n_r = n$ to demonstrate this.

With i.i.d. Rayleigh fading, the capacity of this channel is (cf. (8.15))

$$C_{nn}(\mathsf{SNR}) = \mathbb{E}\left[\sum_{i=1}^{n} \log\left(1 + \mathsf{SNR}\frac{\lambda_i^2}{n}\right)\right], \qquad (8.22)$$

where we emphasize the dependence on n and SNR in the notation. The $\lambda_i/\sqrt{n}$ are the singular values of the random matrix $\mathbf{H}/\sqrt{n}$. By a random matrix result

due to Marčenko and Pastur [78], the empirical distribution of the singular values of $\mathbf{H}/\sqrt{n}$ converges to a deterministic limiting distribution for almost all realizations of $\mathbf{H}$. Figure 8.4 demonstrates the convergence. The limiting distribution is the so-called *quarter circle law*.[3] The corresponding limiting density of the *squared* singular values is given by

$$f^*(x) = \begin{cases} \frac{1}{\pi}\sqrt{\frac{1}{x} - \frac{1}{4}} & 0 \leq x \leq 4, \\ 0 & \text{else.} \end{cases} \tag{8.23}$$

Hence, we can conclude that, for increasing n,

$$\frac{1}{n}\sum_{i=1}^{n}\log\left(1 + \mathsf{SNR}\frac{\lambda_i^2}{n}\right) \to \int_0^4 \log(1 + \mathsf{SNR}x)f^*(x)\mathrm{d}x. \tag{8.24}$$

If we denote

$$c^*(\mathsf{SNR}) := \int_0^4 \log(1 + \mathsf{SNR}x)f^*(x)\mathrm{d}x, \tag{8.25}$$
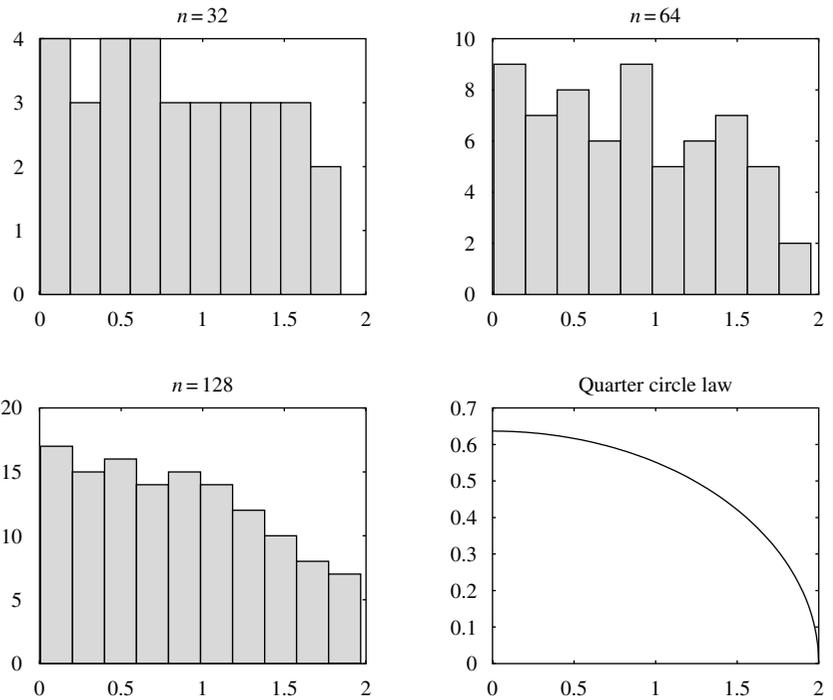
Figure 8.4 Convergence of the empirical singular value distribution of $\mathbf{H}/\sqrt{n}$. For each n, a single random realization of $\mathbf{H}/\sqrt{n}$ is generated and the empirical distribution (histogram) of the singular values is plotted. We see that as n grows, the histogram converges to the quarter circle law.

---

[3] Note that although the singular values are unbounded, in the limit they lie in the interval $[0, 2]$ with probability 1.

we can solve the integral for the density in (8.23) to arrive at (see Exercise 8.17)

$$c^*(\text{SNR}) = 2\log\left(1 + \text{SNR} - \frac{1}{4}F(\text{SNR})\right) - \frac{\log e}{4\text{SNR}}F(\text{SNR}), \tag{8.26}$$

where

$$F(\text{SNR}) := \left(\sqrt{4\text{SNR}+1} - 1\right)^2. \tag{8.27}$$

The significance of $c^*(\text{SNR})$ is that

$$\lim_{n\to\infty}\frac{C_{nn}(\text{SNR})}{n} = c^*(\text{SNR}). \tag{8.28}$$

So capacity grows linearly in n at *any* SNR and the constant $c^*(\text{SNR})$ is the rate of the growth.

We compare the large-n approximation

$$\boxed{C_{nn}(\text{SNR}) \approx nc^*(\text{SNR}),} \tag{8.29}$$

with the actual value of the capacity for $n = 2, 4$ in Figure 8.5. We see the approximation is very good, even for such small values of n. In Exercise 8.7, we see statistical models other than i.i.d. Rayleigh, which also have a linear increase in capacity with an increase in n.

Linear scaling: a more in-depth look

To better understand why the capacity scales linearly with the number of antennas, it is useful to contrast the MIMO scenario here with three other scenarios:
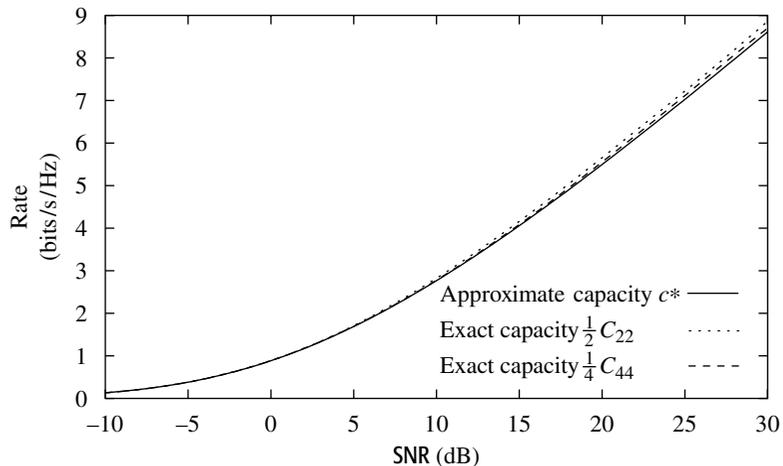
Figure 8.5 Comparison between the large-n approximation and the actual capacity for $n = 2, 4$.

- **MISO channel with a large transmit antenna array** Specializing (8.15) to the n by 1 MISO channel yields the capacity

$$C_{n1} = \mathbb{E}\left[\log\left(1 + \frac{\mathsf{SNR}}{n}\sum_{i=1}^{n}|h_i|^2\right)\right] \text{ bits/s/Hz.} \tag{8.30}$$

As $n \to \infty$, by the law of large numbers,

$$C_{n1} \to \log(1 + \mathsf{SNR}) = C_{\text{awgn}}. \tag{8.31}$$

For $n = 1$, the 1 by 1 fading channel (with only receiver CSI) has lower capacity than the AWGN channel; this is due to the "Jensen's loss" (Section 5.4.5). But recall from Figure 5.20 that this loss is not large for the entire range of SNR. Increasing the number of transmit antennas has the effect of reducing the fluctuation of the instantaneous SNR

$$\frac{1}{n}\sum_{i=1}^{n}|h_i|^2 \cdot \mathsf{SNR}, \tag{8.32}$$

and hence reducing the Jensen's loss, but the loss was not big to start with, hence the gain is minimal. Since the total transmit power is fixed, the multiple transmit antennas provide neither a power gain nor a gain in spatial degrees of freedom. (In a *slow* fading channel, the multiple transmit antennas provide a diversity gain, but this is not relevant in the fast fading scenario considered here.)

- **SIMO channel with a large receive antenna array** A 1 by n SIMO channel has capacity

$$C_{1n} = \mathbb{E}\left[\log\left(1 + \mathsf{SNR}\sum_{i=1}^{n}|h_i|^2\right)\right]. \tag{8.33}$$

For large n

$$C_{1n} \approx \log(n\mathsf{SNR}) = \log n + \log\mathsf{SNR}, \tag{8.34}$$

i.e., the receive antennas provide a power gain (which increases linearly with the number of receive antennas) and the capacity increases logarithmically with the number of receive antennas. This is quite in contrast to the MISO case: the difference is due to the fact that now there is a linear increase in total *received* power due to a larger receive antenna array. However, the increase in capacity is only *logarithmic* in n; the increase in total received power is all accumulated in the single degree of freedom of the channel. There is power gain but no gain in the spatial degrees of freedom.

   The capacities, as a function of n, are plotted for the SIMO, MISO and MIMO channels in Figure 8.6.

Figure 8.6 Capacities of the *n* by 1 MISO channel, 1 by *n* SIMO channel and the *n* by *n* MIMO channel as a function of *n*, for SNR = 0 dB
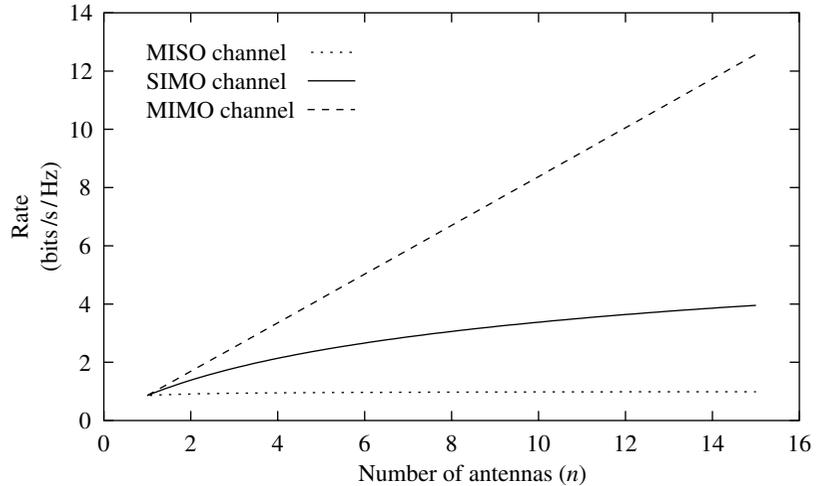
- **AWGN channel with infinite bandwidth** Given a power constraint of $\bar{P}$ and AWGN noise spectral density $N_0/2$, the infinite bandwidth limit is (cf. 5.18)

$$C_\infty = \lim_{W \to \infty} W \log\left(1 + \frac{\bar{P}}{N_0 W}\right) = \frac{\bar{P}}{N_0} \text{ bits/s.} \tag{8.35}$$

Here, although the number of degrees of freedom increases, the capacity remains bounded. This is because the total received power is fixed and hence the SNR per degree of freedom vanishes. There is a gain in the degrees of freedom, but since there is no power gain the received power has to be spread across the many degrees of freedom.

In contrast to all of these scenarios, the capacity of an *n* by *n* MIMO channel increases linearly with *n*, because simultaneously:

- there is a linear increase in the total received power, and
- there is a linear increase in the degrees of freedom, due to the substantial randomness and consequent well-conditionedness of the channel matrix **H**.

Note that the well-conditionedness of the matrix depends on maintaining the uncorrelated nature of the channel gains, $\{h_{ij}\}$, while increasing the number of antennas. This can be achieved in a rich scattering environment by keeping the antenna spacing fixed at half the wavelength and increasing the aperture, *L*, of the antenna array. On the other hand, if we just pack more and more antenna elements in a *fixed* aperture, *L*, then the channel gains will become more and more correlated. In fact, we know from Section 7.3.7 that in the angular domain a MIMO channel with densely spaced antennas and aperture *L* can be reduced to an equivalent 2*L* by 2*L* channel with antennas spaced at half the wavelength. Thus, the number of degrees of freedom is ultimately

limited by the antenna array aperture rather than the number of antenna elements.

8.2.3 Full CSI

We have considered the scenario when only the receiver can track the channel. This is the most interesting case in practice. In a TDD system or in an FDD system where the fading is very slow, it may be possible to track the channel matrix at the transmitter. We shall now discuss how channel capacity can be achieved in this scenario. Although channel knowledge at the transmitter does not help in extracting an additional degree-of-freedom gain, extra power gain is possible.

Capacity

The derivation of the channel capacity in the full CSI scenario is only a slight twist on the time-invariant case discussed in Section 7.1.1. At each time m, we decompose the channel matrix as $\mathbf{H}[m] = \mathbf{U}[m]\mathbf{\Lambda}[m]\mathbf{V}[m]^*$, so that the MIMO channel can be represented as a parallel channel

$$\tilde{y}_i[m] = \lambda_i[m]\tilde{x}_i[m] + \tilde{w}_i[m], \qquad i = 1, \ldots, n_{\min}, \tag{8.36}$$

where $\lambda_1[m] \geq \lambda_2[m] \geq \ldots \geq \lambda_{n_{\min}}[m]$ are the ordered singular values of $\mathbf{H}[m]$ and

$$\begin{aligned}
\tilde{\mathbf{x}}[m] &= \mathbf{V}^*[m]\mathbf{x}[m], \\
\tilde{\mathbf{y}}[m] &= \mathbf{U}^*[m]\mathbf{y}[m], \\
\tilde{\mathbf{w}}[m] &= \mathbf{U}^*[m]\mathbf{w}[m].
\end{aligned}$$

We have encountered the fast fading parallel channel in our study of the single antenna fast fading channel (cf. Section 5.4.6). We allocate powers to the sub-channels based on their strength according to the waterfilling policy

$$P^*(\lambda) = \left(\mu - \frac{N_0}{\lambda^2}\right)^+, \tag{8.37}$$

with μ chosen so that the total transmit power constraint is satisfied:

$$\sum_{i=1}^{n_{\min}} \mathbb{E}\left[\left(\mu - \frac{N_0}{\lambda_i^2}\right)^+\right] = P. \tag{8.38}$$

Note that this is waterfilling over time and space (the eigenmodes). The capacity is given by

$$C = \sum_{i=1}^{n_{\min}} \mathbb{E}\left[\log\left(1 + \frac{P^*(\lambda_i)\lambda_i^2}{N_0}\right)\right]. \tag{8.39}$$

Transceiver architecture

The transceiver architecture that achieves the capacity follows naturally from the SVD-based architecture depicted in Figure 7.2. Information bits are split into $n_{\min}$ parallel streams, each coded separately, and then augmented by $n_t - n_{\min}$ streams of zeros. The symbols across the streams at time m form the vector $\tilde{\mathbf{x}}[m]$. This vector is pre-multiplied by the matrix $\mathbf{V}[m]$ before being sent through the channel, where $\mathbf{H}[m] = \mathbf{U}[m]\mathbf{\Lambda}[m]\mathbf{V}^*[m]$ is the singular value decomposition of the channel matrix at time m. The output is post-multiplied by the matrix $\mathbf{U}^*[m]$ to extract the independent streams, which are then separately decoded. The power allocated to each stream is time-dependent and is given by the waterfilling formula (8.37), and the rates are dynamically allocated accordingly. If an AWGN capacity-achieving code is used for each stream, then the entire system will be capacity-achieving for the MIMO channel.

Performance analysis

Let us focus on the i.i.d. Rayleigh fading model. Since with probability 1, the random matrix $\mathbf{HH}^*$ has full rank (Exercise 8.12), and is, in fact, well-conditioned (Exercise 8.14), it can be shown that at high SNR, the waterfilling strategy allocates an equal amount of power $P/n_{\min}$ to all the spatial modes, as well as an equal amount of power over time. Thus,

$$C \approx \sum_{i=1}^{n_{\min}} \mathbb{E}\left[\log\left(1 + \frac{\mathsf{SNR}}{n_{\min}}\lambda_i^2\right)\right], \tag{8.40}$$

where $\mathsf{SNR} = P/N_0$. If we compare this to the capacity (8.16) with only receiver CSI, we see that the number of degrees of freedom is the same ($n_{\min}$) but there is a power gain of a factor of $n_t/n_{\min}$ when the transmitter can track the channel. Thus, whenever there are more transmit antennas then receive antennas, there is a power boost of n_t/n_r from having transmitter CSI. The reason is simple. Without channel knowledge at the transmitter, the transmit energy is spread out equally across all directions in $\mathcal{C}^{n_t}$. With transmitter CSI, the energy can now be focused on only the n_r non-zero eigenmodes, which form a subspace of dimension n_r inside $\mathcal{C}^{n_t}$. For example, with $n_r = 1$, the capacity with only receiver CSI is

$$\mathbb{E}\left[\log\left(1 + \mathsf{SNR}/n_t \sum_{i=1}^{n_t} |h_i|^2\right)\right],$$

while the high SNR capacity when there is full CSI is

$$\mathbb{E}\left[\log\left(1 + \mathsf{SNR}\sum_{i=1}^{n_t} |h_i|^2\right)\right].$$

Thus a power gain of a factor of n_t is achieved by transmit beamforming. With dual transmit antennas, this is a gain of 3 dB.

At low SNR, there is a further gain from transmitter CSI due to dynamic allocation of power across the eigenmodes: at any given time, more power is given to stronger eigenmodes. This gain is of the same nature as the one from opportunistic communication discussed in Chapter 6.

What happens in the large antenna array regime? Applying the random matrix result of Marčenko and Pastur from Section 8.2.2, we conclude that the random singular values $\lambda_i[m]/\sqrt{n}$ of the channel matrix $\mathbf{H}[m]/\sqrt{n}$ converge to the same deterministic limiting distribution f^* across all times m. This means that in the waterfilling strategy, there is no dynamic power allocation over time, only over space. This is sometimes known as a *channel hardening* effect.

Summary 8.1 Performance gains in a MIMO channel

The capacity of an $n_t \times n_r$ i.i.d. Rayleigh fading MIMO channel $\mathbf{H}$ with receiver CSI is

$$C_{nn}(\text{SNR}) = \mathbb{E}\left[\log\det\left(\mathbf{I}_{n_r} + \frac{\text{SNR}}{n_t}\mathbf{H}\mathbf{H}^*\right)\right]. \qquad (8.41)$$

At high SNR, the capacity is approximately equal (up to an additive constant) to $n_{\min}\log\text{SNR}$ bits/s/Hz.

At low SNR, the capacity is approximately equal to $n_r\,\text{SNR}\log_2 e$ bits/s/Hz, so only a receive beamforming gain is realized.

With $n_t = n_r = n$, the capacity can be approximated by $nc^*(\text{SNR})$ where $c^*(\text{SNR})$ is the constant in (8.26).

Conclusion: In an $n \times n$ MIMO channel, the capacity increases *linearly* with n over the entire SNR range.

With channel knowledge at the transmitter, an additional n_t/n_r-fold transmit beamforming gain can be realized with an additional power gain from temporal–spatial waterfilling at low SNR.

8.3 Receiver architectures

The transceiver architecture of Figure 8.1 achieves the capacity of the fast fading MIMO channel with receiver CSI. The capacity is achieved by joint ML decoding of the data streams at the receiver, but the complexity grows exponentially with the number of data streams. Simpler decoding rules that provide soft information to feed to the decoders of the individual data streams is an active area of research; some of the approaches are reviewed

in Exercise 8.15. In this section, we consider receiver architectures that use *linear* operations to convert the problem of joint decoding of the data streams into one of individual decoding of the data streams. These architectures extract the spatial degree of freedom gains characterized in the previous section. In conjunction with successive cancellation of data streams, we can achieve the capacity of the fast fading MIMO channel. To be able to focus on the receiver design, we start with transmitting the independent data streams directly over the antenna array (i.e., $\mathbf{Q} = \mathbf{I}_{n_t}$ in Figure 8.1).

8.3.1 Linear decorrelator

Geometric derivation

Is it surprising that the full degrees of freedom of $\mathbf{H}$ can be attained even when the transmitter does not track the channel matrix? When the transmitter does know the channel, the SVD architecture enables the transmitter to send parallel data streams through the channel so that they arrive orthogonally at the receiver without interference between the streams. This is achieved by pre-rotating the data so that the parallel streams can be sent along the eigenmodes of the channel. When the transmitter does not know the channel, this is not possible. Indeed, after passing through the MIMO channel of (7.1), the independent data streams sent on the transmit antennas all arrive cross-coupled at the receiver. It is not clear a priori that the receiver can separate the data streams efficiently enough so that the resulting performance has full degrees of freedom. But in fact we have already seen such a receiver: the channel inversion receiver in the 2×2 example discussed in Section 3.3.3. We develop the structure of this receiver in full generality here.

To simplify notations, let us first focus on the time-invariant case, where the channel matrix is fixed. We can write the received vector at symbol time m as

$$\mathbf{y}[m] = \sum_{i=1}^{n_t} \mathbf{h}_i x_i[m] + \mathbf{w}[m], \qquad (8.42)$$

where $\mathbf{h}_1, \ldots, \mathbf{h}_{n_t}$ are the columns of $\mathbf{H}$ and the data streams transmitted on the antennas, $\{x_i[m]\}$ on the ith antenna, are all independent. Focusing on the kth data stream, we can rewrite (8.42):

$$\mathbf{y}[m] = \mathbf{h}_k x_k[m] + \sum_{i \neq k} \mathbf{h}_i x_i[m] + \mathbf{w}. \qquad (8.43)$$

Compared to the SIMO point-to-point channel from Section 7.2.1, we see that the kth data stream faces an extra source of interference, that from the other data streams. One idea that can be used to remove this inter-stream interference is to project the received signal $\mathbf{y}$ onto the subspace orthogonal to the one spanned by the vectors $\mathbf{h}_1, \ldots, \mathbf{h}_{k-1}, \mathbf{h}_{k+1}, \ldots, \mathbf{h}_{n_t}$

(denoted henceforth by V_k). Suppose that the dimension of V_k is d_k. Projection is a linear operation and we can represent it by a d_k by n_r matrix $\mathbf{Q}_k$, the rows of which form an orthonormal basis of V_k; they are all orthogonal to $\mathbf{h}_1, \ldots, \mathbf{h}_{k-1}, \mathbf{h}_{k+1}, \ldots, \mathbf{h}_{n_t}$. The vector $\mathbf{Q}_k \mathbf{v}$ should be interpreted as the projection of the vector $\mathbf{v}$ onto V_k, but expressed in terms of the coordinates defined by the basis of V_k formed by the rows of $\mathbf{Q}_k$. A pictorial depiction of this projection operation is in Figure 8.7.

Now, the inter-stream interference "nulling" is successful (that is, the resulting projection of $\mathbf{h}_k$ is a non-zero vector) if the kth data stream "spatial signature" $\mathbf{h}_k$ is not a linear combination of the spatial signatures of the other data streams. In other words, if there are more data streams than the dimension of the received signal (i.e., $n_t > n_r$), then the nulling operation will not be successful, even for a full rank $\mathbf{H}$. Hence, we should choose the number of data streams to be no more than n_r. Physically, this corresponds to using only a subset of the transmit antennas and for notational convenience we will count only the transmit antennas that are used, by just making the assumption $n_t \leq n_r$ in the decorrelator discussion henceforth.

After the projection operation,

$$\tilde{\mathbf{y}}[m] := \mathbf{Q}_k \mathbf{y}[m] = \mathbf{Q}_k \mathbf{h}_k \mathbf{x}_k[m] + \tilde{\mathbf{w}}[m]$$

where $\tilde{\mathbf{w}}[m] := \mathbf{Q}_k \mathbf{w}[m]$ is the noise, still white, after the projection. Optional demodulation of the kth stream can now be performed by match filtering to the vector $\mathbf{Q}_k \mathbf{h}_k$. The output of this matched filter (or maximal ratio combiner) has SNR

$$\frac{P_k \|\mathbf{Q}_k \mathbf{h}_k\|^2}{N_0}, \tag{8.44}$$

where P_k is the power allocated to stream k.
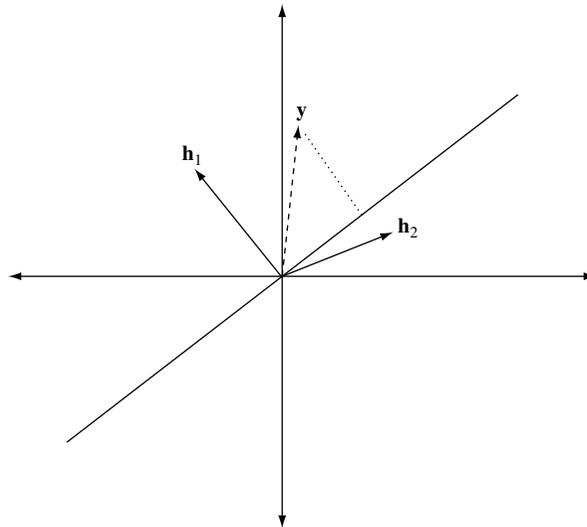
Figure 8.7 A schematic representation of the projection operation: $\mathbf{y}$ is projected onto the subspace orthogonal to $\mathbf{h}_1$ to demodulate stream 2.

The combination of the projection operation followed by the matched filter is called the *decorrelator* (also known as *interference nulling* or *zero-forcing* receiver). Since projection and matched filtering are both linear operations, the decorrelator is a linear filter. The filter $\mathbf{c}_k$ is given by

$$\mathbf{c}_k^* = (\mathbf{Q}_k \mathbf{h}_k)^* \mathbf{Q}_k, \tag{8.45}$$

or

$$\mathbf{c}_k = (\mathbf{Q}_k^* \mathbf{Q}_k) \mathbf{h}_k, \tag{8.46}$$

which is the projection of $\mathbf{h}_k$ onto the subspace V_k, expressed in terms of the original coordinates. Since the matched filter maximizes the output SNR, the decorrelator can also be interpreted as the linear filter that maximizes the output SNR subject to the constraint that the filter nulls out the interference from all other streams. Intuitively, we are projecting the received signal in the direction within V_k that is closest to $\mathbf{h}_k$.

Only the kth stream has been in focus so far. We can now decorrelate each of the streams separately, as illustrated in Figure 8.8. We have described the decorrelator geometrically; however, there is a simple explicit formula for the entire bank of decorrelators: the decorrelator for the kth stream is the kth column of the pseudoinverse $\mathbf{H}^\dagger$ of the matrix $\mathbf{H}$, defined by

$$\mathbf{H}^\dagger := (\mathbf{H}^* \mathbf{H})^{-1} \mathbf{H}^*. \tag{8.47}$$
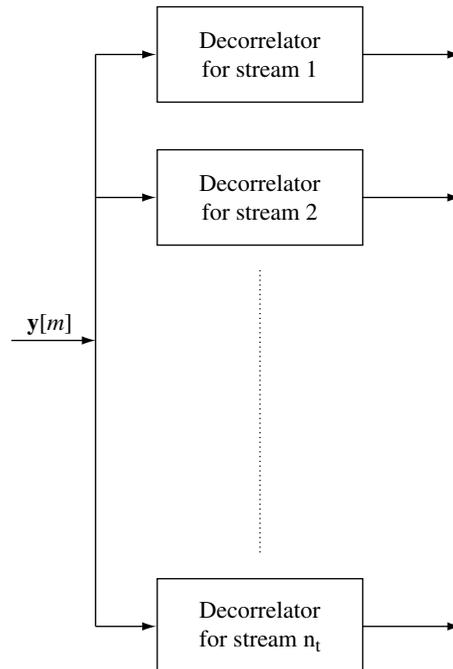
Figure 8.8 A bank of decorrelators, each estimating the parallel data streams.

The validity of this formula is verified in Exercise 8.11. In the special case when $\mathbf{H}$ is square and invertible, $\mathbf{H}^\dagger = \mathbf{H}^{-1}$ and the decorrelator is precisely the channel inversion receiver we already discussed in Section 3.3.3.

Performance for a deterministic $\mathbf{H}$

The channel from the kth stream to the output of the corresponding decorrelator is a Gaussian channel with SNR given by (8.44). A Gaussian code achieves the maximum data rate, given by

$$C_k := \log\left(1 + \frac{P_k\|\mathbf{Q}_k\mathbf{h}_k\|^2}{N_0}\right). \tag{8.48}$$

To get a better feel for this performance, let us compare it with the ideal situation of no inter-stream interference in (8.43). As we observed above, if there were no inter-stream interference in (8.43), the situation is exactly the SIMO channel of Section 7.2.1; the filter would be matched to $\mathbf{h}_k$ and the achieved SNR would be

$$\frac{P_k\|\mathbf{h}_k\|^2}{N_0}. \tag{8.49}$$

Since the inter-stream interference only hampers the recovery of the kth stream, the performance of the decorrelator (in terms of the SNR in (8.44)) must in general be less than that achieved by a matched filter with no inter-stream interference. We can also see this explicitly: the projection operation cannot increase the length of a vector and hence $\|\mathbf{Q}_k\mathbf{h}_k\| \leq \|\mathbf{h}_k\|$. We can further say that the projection operation always reduces the length of $\mathbf{h}_k$ unless $\mathbf{h}_k$ is already orthogonal to the spatial signatures of the other data streams.

Let us return to the bank of decorrelators in Figure 8.8. The total rate of communication supported here with efficient coding in each of the data streams is the sum of the individual rates in (8.48) and is given by

$$\sum_{k=1}^{n_t} C_k.$$

Performance in fading channels

So far our analysis has focused on a deterministic channel $\mathbf{H}$. As usual, in the time-varying fast fading scenario, coding should be done over time across the different fades, usually in combination with interleaving. The maximum achievable rate can be computed by simply averaging over the stationary distribution of the channel process $\{\mathbf{H}[m]\}_m$, yielding

$$R_{\text{decorr}} = \sum_{k=1}^{n_t} \bar{C}_k, \tag{8.50}$$

where

$$\bar{C}_k = \mathbb{E}\left[\log\left(1 + \frac{P_k\|\mathbf{Q}_k\mathbf{h}_k\|^2}{N_0}\right)\right]. \tag{8.51}$$

The achievable rate in (8.50) is in general less than or equal to the capacity of the MIMO fading channel with CSI at the receiver (cf. (8.10)) since transmission using independent data streams and receiving using the bank of decorrelators is only one of several possible communication strategies. To get some further insight, let us look at a specific statistical model, that of i.i.d. Rayleigh fading. Motivated by the fact that the optimal covariance matrix is of the form of scaled identity (cf. (8.12)), let us choose equal powers for each of the data streams (i.e., $P_k = P/n_t$). Continuing from (8.50), the decorrelator bank performance specialized to i.i.d. Rayleigh fading is (recall that for successful decorrelation $n_{\min} = n_t$)

$$R_{\text{decorr}} = \mathbb{E}\left[\sum_{k=1}^{n_{\min}} \log\left(1 + \frac{\text{SNR}}{n_t}\|\mathbf{Q}_k\mathbf{h}_k\|^2\right)\right]. \tag{8.52}$$

Since $\mathbf{h}_k \sim \mathcal{CN}(0, \mathbf{I}_{n_r})$, we know that $\|\mathbf{h}_k\|^2 \sim \chi^2_{2n_r}$, where χ^2_{2i} is a χ-squared random variable with $2i$ degrees of freedom (cf. (3.36)). Here $\mathbf{Q}_k\mathbf{h}_k \sim \mathcal{CN}(0, \mathbf{I}_{\dim V_k})$ (since $\mathbf{Q}_k\mathbf{Q}_k^* = \mathbf{I}_{\dim V_k}$). It can be shown that the channel $\mathbf{H}$ is full rank with probability 1 (see Exercise 8.12), and this means that $\dim V_k = n_r - n_t + 1$ (see Exercise 8.13). Thus $\|\mathbf{Q}_k\mathbf{h}_k\|^2 \sim \chi^2_{2(n_r-n_t+1)}$. This provides us with an explicit example for our earlier observation that the projection operation reduces the length. In the special case of a square system, $\dim V_k = 1$, and $\mathbf{Q}_k\mathbf{h}_k$ is a scalar distributed as circular symmetric Gaussian; we have already seen this in the 2×2 example of Section 3.3.3.

R_{decorr} is plotted in Figure 8.9 for different numbers of antennas. We see that the asymptotic slope of the rate obtained by the decorrelator bank as a
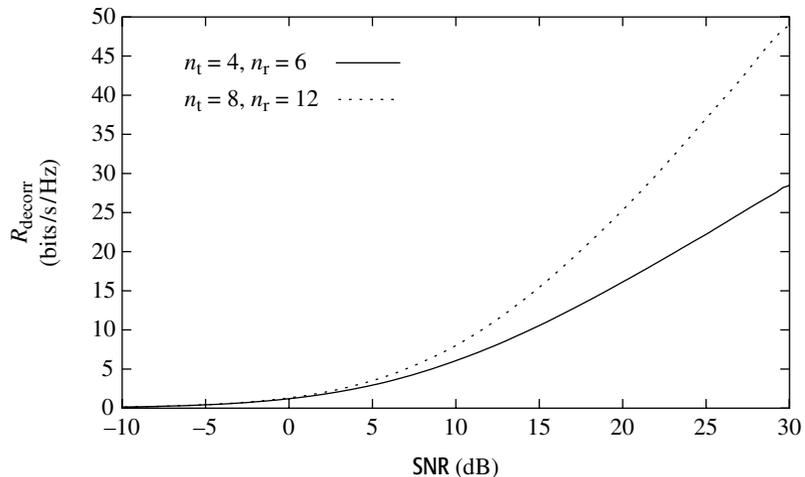
Figure 8.9 Rate achieved (in bits/s/Hz) by the decorrelator bank.

function of SNR in dB is proportional to $n_{\min}$; the same slope in the capacity of the MIMO channel. More specifically, we can approximate the rate in (8.52) at high SNR as

$$R_{\text{decorr}} \approx n_{\min} \log \frac{\text{SNR}}{n_{\text{t}}} + \mathbb{E}\left[\sum_{k=1}^{n_{\text{t}}} \log\left(\|\mathbf{Q}_k \mathbf{h}_k\|^2\right)\right], \tag{8.53}$$

$$= n_{\min} \log\left(\frac{\text{SNR}}{n_{\text{t}}}\right) + n_{\text{t}} \mathbb{E}\left[\log \chi^2_{2(n_{\text{r}}-n_{\text{t}}+1)}\right]. \tag{8.54}$$

Comparing (8.53) and (8.54) with the corresponding high SNR expansion of the capacity of this MIMO channel (cf. (8.18) and (8.20)), we can make the following observations:

- The first-order term (in the high SNR expansion) is the same for both the rate achieved by the decorrelator bank and the capacity of the MIMO channel. Thus, the decorrelator bank is able to fully harness the spatial degrees of freedom of the MIMO channel.
- The next term in the high SNR expansion (constant term) shows the performance degradation, in rate, of using the decorrelator bank as compared to the capacity of the channel. Figure 8.10 highlights this difference in the special case of $n_{\text{t}} = n_{\text{r}} = n$.

The above analysis is for the high SNR regime. At any *fixed* SNR, it is also straightforward to show that, just like the capacity, the total rate achievable by the bank of decorrelators scales linearly with the number of antennas (see Exercise 8.21).
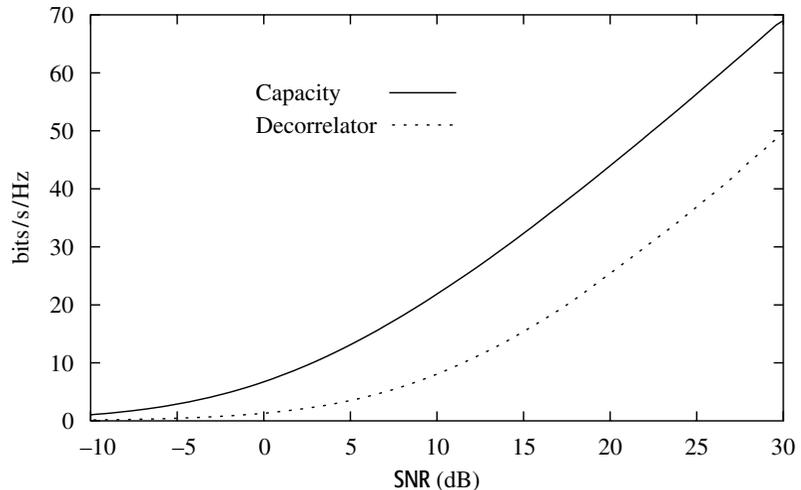
Figure 8.10 Plot of rate achievable with the decorrelator bank for the $n_{\text{t}} = n_{\text{r}} = 8$ i.i.d. Rayleigh fading channel. The capacity of the channel is also plotted for comparison.

8.3.2 Successive cancellation

We have just considered a bank of *separate* filters to estimate the data streams. However, the result of one of the filters could be used to aid the operation of the others. Indeed, we can use the *successive cancellation* strategy described in the uplink capacity analysis (in Section 6.1): once a data stream is successfully recovered, we can subtract it off from the received vector and reduce the burden on the receivers of the remaining data streams. With this motivation, consider the following modification to the bank of separate receiver structures in Figure 8.8. We use the first decorrelator to decode the data stream $x_1[m]$ and then subtract off this decoded stream from the received vector. If the first stream is successfully decoded, then the second decorrelator has to deal only with streams $x_3, \ldots, x_{n_t}$ as interference, since x_1 has been correctly subtracted off. Thus, the second decorrelator projects onto the subspace orthogonal to that spanned by $\mathbf{h}_3, \ldots, \mathbf{h}_{n_t}$. This process is continued until the final decorrelator does not have to deal with any interference from the other data streams (assuming successful subtraction in each preceding stage). This decorrelator–SIC (decorrelator with successive interference cancellation) architecture is illustrated in Figure 8.11.

One problem with this receiver structure is *error propagation*: an error in decoding the kth data stream means that the subtracted signal is incorrect and this error propagates to all the streams further down, $k+1, \ldots, n_t$. A careful analysis of the performance of this scheme is complicated, but can be made easier if we take the data streams to be well coded and the block length to be very large, so that streams are successfully cancelled with very high probability. With this assumption the kth data stream sees only down-stream interference, i.e., from the streams $k+1, \ldots, n_t$. Thus,
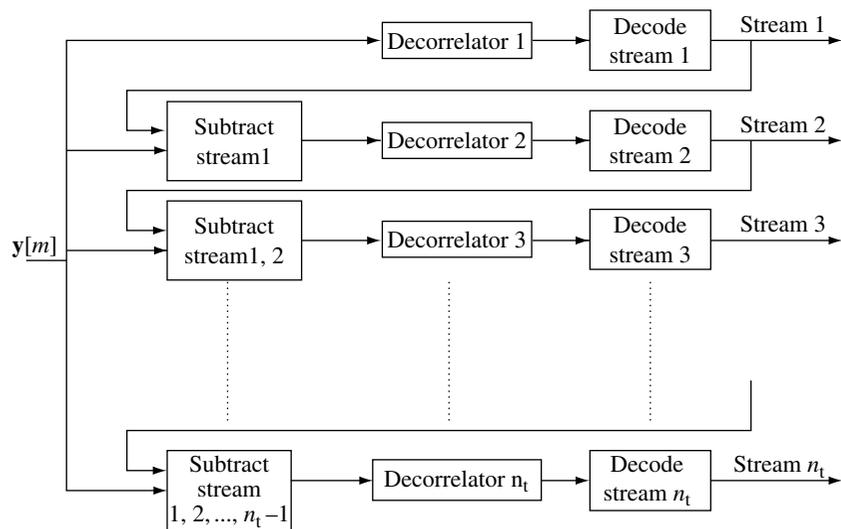
Figure 8.11 Decorrelator–SIC: A bank of decorrelators with successive cancellation of streams.

the corresponding projection operation (denoted by $\tilde{\mathbf{Q}}_k$) is onto a higher dimensional subspace (one orthogonal to that spanned by $\mathbf{h}_{k+1}, \ldots, \mathbf{h}_{n_t}$, as opposed to being orthogonal to the span of $\mathbf{h}_1, \ldots, \mathbf{h}_{k-1}, \mathbf{h}_{k+1}, \ldots, \mathbf{h}_{n_t}$). As in the calculation of the previous section, the SNR of the kth data stream is (cf. (8.44))

$$\frac{P_k \| \tilde{\mathbf{Q}}_k \mathbf{h}_k \|^2}{N_0}. \tag{8.55}$$

While we clearly expect this to be an improvement over the simple bank of decorrelators, let us again turn to the i.i.d. Rayleigh fading model to see this concretely. Analogous to the high SNR expansion of (8.52) in (8.53) for the simple decorrelator bank, with SIC and equal power allocation to each stream, we have

$$R_{\mathrm{dec-sic}} \approx n_{\min} \log \frac{\mathsf{SNR}}{n_t} + \mathbb{E}\left[\sum_{k=1}^{n_t} \log(\| \tilde{\mathbf{Q}}_k \mathbf{h}_k \|^2) \right]. \tag{8.56}$$

Similar to our analysis of the basic decorrelator bank, we can argue that $\| \tilde{\mathbf{Q}}_k \mathbf{h}_k \|^2 \sim \chi^2_{2(n_r - n_t + k)}$ with probability 1 (cf. Exercise 8.13), thus arriving at

$$\mathbb{E}\left[\log(\| \tilde{\mathbf{Q}}_k \mathbf{h}_k \|^2) \right] = \mathbb{E}[\log \chi^2_{2(n_r - n_t + k)}]. \tag{8.57}$$

Comparing this rate at high SNR with both the simple decorrelator bank and the capacity of the channel (cf. (8.53) and (8.18)), we observe the following

- The first-order term in the high SNR expansion is the same as that in the rate of the decorrelator bank and in the capacity: successive cancellation does not provide additional degrees of freedom.
- Moving to the next (constant) term, we see the performance boost in using the decorrelator–SIC over the simple decorrelator bank: the improved constant term is now *equal* to that in the capacity expansion. This boost in performance can be viewed as a *power gain*: by *decoding and subtracting* instead of *linear nulling*, the effective SNR at each stage is improved.

8.3.3 Linear MMSE receiver

Limitation of the decorrelator

We have seen the performance of the basic decorrelator bank and the decorrelator–SIC. At high SNR, for i.i.d. Rayleigh fading, the basic decorrelator bank achieves the full degrees of freedom in the channel. With SIC even the constant term in the high SNR capacity expansion is achieved. What about low SNR? The performance of the decorrelator bank (both with and without the modification of successive cancellation) as compared to the capacity of the MIMO channel is plotted in Figure 8.12.

Figure 8.12 Performance of
the decorrelator bank, with
and without successive
cancellation at low SNR. Here
$n_t = n_r = 8$.
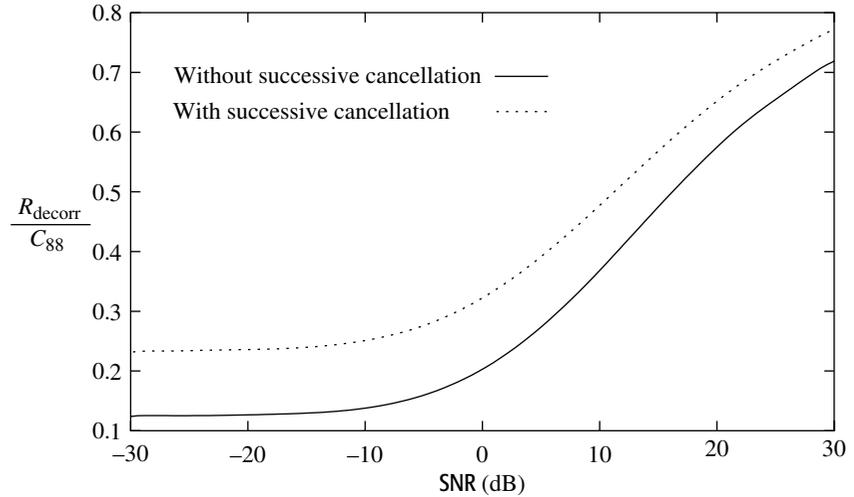
The main observation is that while the decorrelator bank performs well at
high SNR, it is really far away from the capacity at low SNR. What is going
on here?

To get more insight, let us plot the performance of a bank of matched
filters, the kth filter being matched to the spatial signature $\mathbf{h}_k$ of transmit
antenna k. From Figure 8.13 we see that the performance of the bank of
matched filters is far superior to the decorrelator bank at low SNR (although
far inferior at high SNR).

Derivation of the MMSE receiver

The decorrelator was motivated by the fact that it completely nulls out inter-
stream interference; in fact it maximizes the output SNR among all linear

Figure 8.13 Performance (ratio
of the rate to the capacity) of
the matched filter bank as
compared to that of the
decorrelator bank. At low SNR,
the matched filter is superior.
The opposite is true for the
decorrelator. The channel is
i.i.d. Rayleigh with $n_t = n_r = 8$.
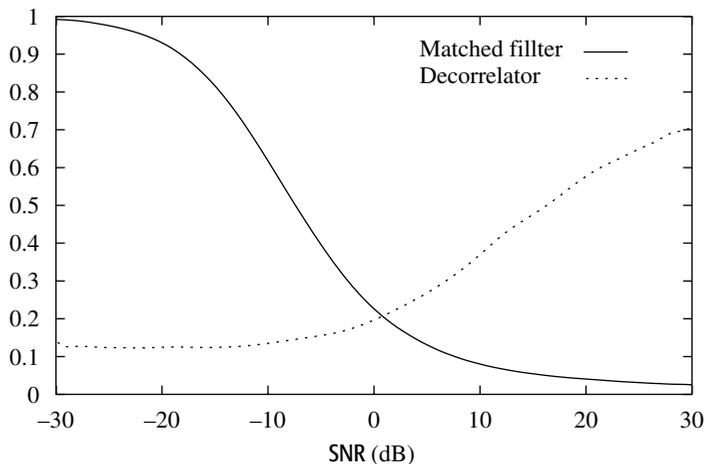
receivers that completely null out the interference. On the other hand, matched filtering (maximal ratio combining) is the optimal strategy for SIMO channels without any inter-stream interference. We called this *receive beamforming* in Example 1 in Section 7.2.1. Thus, we see a tradeoff between completely eliminating inter-stream interference (without any regard to how much energy of the stream of interest is lost in this process) and preserving as much energy content of the stream of interest as possible (at the cost of possibly facing high inter-stream interference). The decorrelator and the matched filter operate at two extreme ends of this tradeoff. At high SNR, the inter-stream interference is dominant over the additive Gaussian noise and the decorrelator performs well. On the other hand, at low SNR the inter-stream interference is not as much of an issue and receive beamforming (matched filter) is the superior strategy. In fact, the bank of matched filters achieves capacity at low SNR (Exercise 8.20).

We can ask for a linear receiver that *optimally* trades off fighting inter-stream interference and the background Gaussian noise, i.e., the receiver that maximizes the output signal-to-interference-plus-noise ratio (SINR) for any value of SNR. Such a receiver looks like the decorrelator when the inter-stream interference is large (i.e., when SNR is large) and like the matched filter when the interference is small (i.e., when SNR is small) (Figure 8.14). This can be thought of as the natural generalization of receive beamforming to the case when there is interference as well as noise.

To formulate this tradeoff precisely, let us first look at the following generic vector channel:

$$\mathbf{y} = \mathbf{h}x + \mathbf{z}, \tag{8.58}$$

where $\mathbf{z}$ is complex circular symmetric colored noise with an invertible covariance matrix $\mathbf{K}_z$, $\mathbf{h}$ is a deterministic vector and x is the unknown scalar symbol
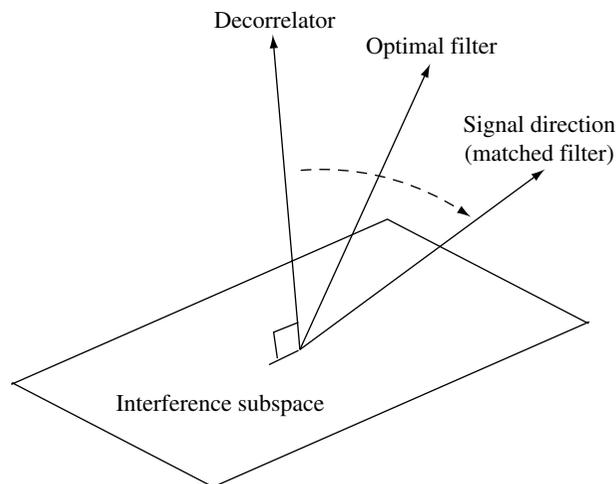
Figure 8.14 The optimal filter goes from being the decorrelator at high SNR to being the matched filter at low SNR.

to be estimated. $\mathbf{z}$ and x are assumed to be uncorrelated. We would like to choose a filter with maximum output SNR. If the noise is white, we know that it is optimal to project $\mathbf{y}$ onto the direction along $\mathbf{h}$. This observation suggests a natural strategy for the colored noise situation: first whiten the noise, and then follow the strategy used with white additive noise. That is, we first pass $\mathbf{y}$ through the invertible[4] linear transformation $\mathbf{K}_z^{-\frac{1}{2}}$ such that the noise $\tilde{\mathbf{z}} := \mathbf{K}_z^{-\frac{1}{2}}\mathbf{z}$ becomes white:

$$\mathbf{K}_z^{-\frac{1}{2}}\mathbf{y} = \mathbf{K}_z^{-\frac{1}{2}}\mathbf{h}x + \tilde{\mathbf{z}}. \tag{8.59}$$

Next, we project the output in the direction of $\mathbf{K}_z^{-\frac{1}{2}}\mathbf{h}$ to get an effective scalar channel

$$(\mathbf{K}_z^{-\frac{1}{2}}\mathbf{h})^*\mathbf{K}_z^{-\frac{1}{2}}\mathbf{y} = \mathbf{h}^*\mathbf{K}_z^{-1}\mathbf{y} = \mathbf{h}^*\mathbf{K}_z^{-1}\mathbf{h}x + \mathbf{h}^*\mathbf{K}_z^{-1}\mathbf{z}. \tag{8.60}$$

Thus the linear receiver in (8.60), represented by the vector

$$\boxed{\mathbf{v}_{\mathrm{mmse}} := \mathbf{K}_z^{-1}\mathbf{h},} \tag{8.61}$$

maximizes the SNR. It can also be shown that this receiver, with an appropriate scaling, minimizes the mean square error in estimating x (see Exercise 8.18), and hence it is also called the linear MMSE (minimum mean squared error) receiver. The corresponding SINR achieved is

$$\sigma_x^2\mathbf{h}^*\mathbf{K}_z^{-1}\mathbf{h}. \tag{8.62}$$

We can now upgrade the receiver structure in Section 8.3.1 by replacing the decorrelator for each stream by the linear MMSE receiver. Again, let us first consider the case where the channel $\mathbf{H}$ is fixed. The effective channel for the kth stream is

$$\mathbf{y}[m] = \mathbf{h}_k x_k[m] + \mathbf{z}_k[m], \tag{8.63}$$

where $\mathbf{z}_k$ represents the noise plus interference faced by data stream k:

$$\mathbf{z}_k[m] := \sum_{i \neq k}\mathbf{h}_i x_i[m] + \mathbf{w}[m]. \tag{8.64}$$

---

[4] $\mathbf{K}_z$ is an invertible covariance matrix and so it can be written as $\mathbf{U}\Lambda\mathbf{U}^*$ for rotation matrix $\mathbf{U}$ and diagonal matrix Λ with positive diagonal elements. Now $\mathbf{K}_z^{\frac{1}{2}}$ is defined as $\mathbf{U}\Lambda^{\frac{1}{2}}\mathbf{U}^*$, with $\Lambda^{\frac{1}{2}}$ defined as a diagonal matrix with diagonal elements equal to the square root of the diagonal elements of Λ.

With power P_i associated with the data stream i, we can explicitly calculate the covariance of $\mathbf{z}_k$

$$\mathbf{K}_{z_k} := N_0 \mathbf{I}_{n_r} + \sum_{i \neq k}^{n_t} P_i \mathbf{h}_i \mathbf{h}_i^*, \tag{8.65}$$

and also note that the covariance is invertible. Substituting this expression for the covariance matrix into (8.61) and (8.62), we see that the linear receiver in the kth stage is given by

$$\left(N_0 \mathbf{I}_{n_r} + \sum_{i \neq k}^{n_t} P_i \mathbf{h}_i \mathbf{h}_i^* \right)^{-1} \mathbf{h}_k, \tag{8.66}$$

and the corresponding output SINR is

$$P_k \mathbf{h}_k^* \left(N_0 \mathbf{I}_{n_r} + \sum_{i \neq k}^{n_t} P_i \mathbf{h}_i \mathbf{h}_i^* \right)^{-1} \mathbf{h}_k. \tag{8.67}$$

Performance

We motivated the design of the linear MMSE receiver as something in between the decorrelator and receiver beamforming. Let us now see this explicitly. At very low SNR (i.e., $P_1, \ldots, P_{n_t}$ are very small compared to N_0) we see that

$$\mathbf{K}_{z_k} \approx N_0 \mathbf{I}_{n_r}, \tag{8.68}$$

and the linear MMSE receiver in (8.66) reduces to the matched filter. On the other hand, at high SNR, the $\mathbf{K}_{z_k}^{-\frac{1}{2}}$ operation reduces to the projection of $\mathbf{y}$ onto the subspace orthogonal to that spanned by $\mathbf{h}_1, \ldots, \mathbf{h}_{k-1}, \mathbf{h}_{k+1}, \ldots, \mathbf{h}_{n_t}$ and the linear MMSE receiver reduces to the decorrelator.

Assuming the use of capacity-achieving codes for each stream, the maximum data rate that stream k can reliably carry is

$$C_k = \log \left(1 + P_k \mathbf{h}_k^* \mathbf{K}_{z_k}^{-1} \mathbf{h}_k \right). \tag{8.69}$$

As usual, the analysis directly carries over to the time-varying fading scenario, with data rate of the kth stream being

$$\bar{C}_k = \mathbb{E}[\log(1 + P_k \mathbf{h}_k^* \mathbf{K}_{z_k}^{-1} \mathbf{h}_k)], \tag{8.70}$$

where the average is over the stationary distribution of $\mathbf{H}$.

The performance of a bank of MMSE filters with equal power allocation over an i.i.d. Rayleigh fading channel is plotted in Figure 8.15. We see that the MMSE receiver performs strictly better than both the decorrelator and the matched filter over the entire range of SNRs.

Figure 8.15 Performance (the ratio of rate to the capacity) of a basic bank of MMSE receivers as compared to the matched filter bank and to the decorrelator bank. MMSE performs better than both, over the entire range of SNR. The channel is i.i.d. Rayleigh with $n_t = n_r = 8$.
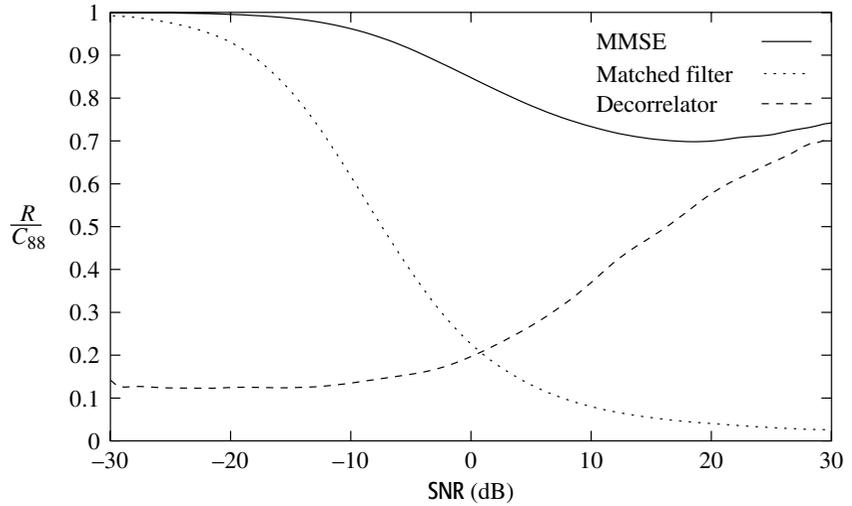
MMSE–SIC

Analogous to what we did in Section 8.3.2 for the decorrelator, we can now upgrade the basic bank of linear MMSE receivers by allowing successive cancellation of streams as well, as depicted in Figure 8.16. What is the performance improvement in using the MMSE–SIC receiver? Figure 8.17 plots the performance as compared to the capacity of the channel (with $n_t = n_r = 8$) for i.i.d. Rayleigh fading. We observe a startling fact: the bank of linear MMSE receivers with successive cancellation and equal power allocation *achieves* the capacity of the i.i.d. Rayleigh fading channel.
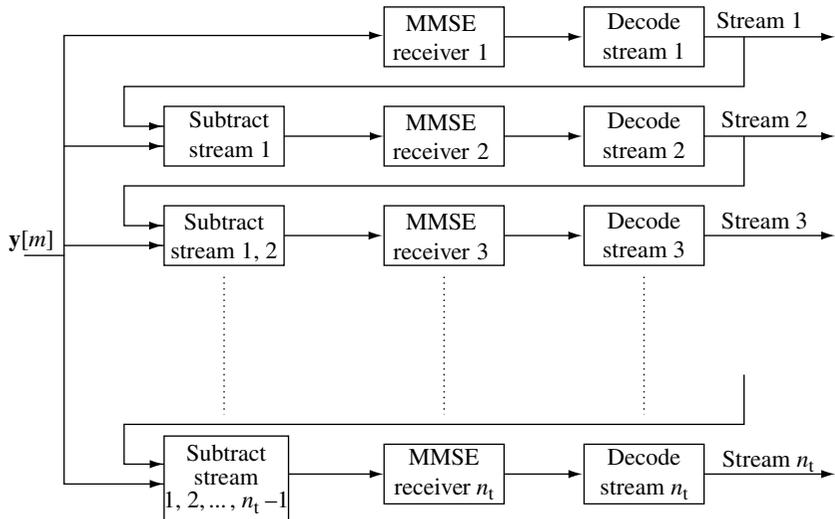
Figure 8.16 MMSE–SIC: a bank of linear MMSE receivers, each estimating one of the parallel data streams, with streams successively cancelled from the received vector at each stage.
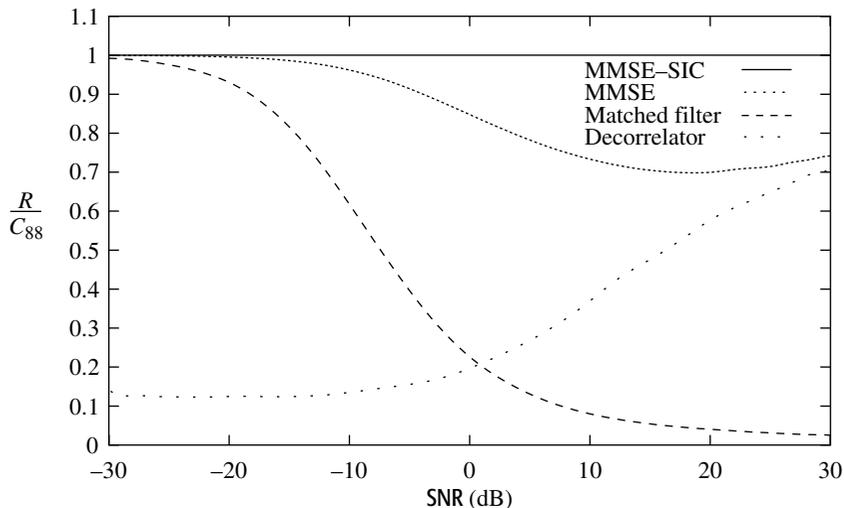
In fact, the MMSE–SIC receiver is optimal in a much stronger sense: it achieves the best possible sum rate (8.2) of the transceiver architecture in Section 8.1 for any given $\mathbf{H}$. That is, if the MMSE–SIC receiver is used for demodulating the streams and the SINR and rate for stream k are SINR_k and $\log(1 + \mathsf{SINR}_k)$ respectively, then the rates sum up to

$$\sum_{k=1}^{n_t} \log(1 + \mathsf{SINR}_k) = \log\det(\mathbf{I}_{n_r} + \mathbf{H}\mathbf{K}_x\mathbf{H}^*), \qquad (8.71)$$

which is the best possible sum rate. While this result can be verified directly by matrix manipulations (Exercise 8.22), the following section gives a deeper explanation in terms of the underlying information theory (the background of which is covered in Appendix B). Understanding at this level will be very useful as we adapt the MMSE–SIC architecture to the analysis of the uplink with multiple antennas in Chapter 10.

8.3.4 Information theoretic optimality*

MMSE is information lossless

As a key step to understanding why the MMSE–SIC receiver is optimal, let us go back to the generic vector channel with additive colored noise (8.58):

$$\mathbf{y} = \mathbf{h}x + \mathbf{z}, \qquad (8.72)$$

---

* This section can be skipped on a first reading. It requires knowledge of material in Appendix B and is not essential for understanding the rest of the book, except for the analysis of the MIMO uplink in Chapter 10.

but now with the further assumption that x and $\mathbf{z}$ are Gaussian. In this case, it can be seen that the linear MMSE filter ($\mathbf{v}_{\text{mmse}} := \mathbf{K}_z^{-1}\mathbf{h}$, cf. (8.61)) not only maximizes the SNR, but also provides a *sufficient statistic* to detect x, i.e., it is information lossless. Thus,

$$I(x; \mathbf{y}) = I(x; \mathbf{v}_{\text{mmse}}^*\mathbf{y}). \tag{8.73}$$

The justification for this step is carried out in Exercise 8.19.

A time-invariant channel

Consider again the MIMO channel with a time-invariant channel matrix $\mathbf{H}$:

$$\mathbf{y}[m] = \mathbf{H}\mathbf{x}[m] + \mathbf{w}[m].$$

We choose the input $\mathbf{x}$ to be $\mathcal{CN}(0, \text{diag}\{P_1, \ldots, P_{n_t}\})$. We can rewrite the mutual information between the input and the output as

$$
\begin{aligned}
I(\mathbf{x}; \mathbf{y}) &= I(x_1, x_2, \ldots, x_{n_t}; \mathbf{y}) \\
&= I(x_1; \mathbf{y}) + I(x_2; \mathbf{y}|x_1) + \cdots + I(x_{n_t}; \mathbf{y}|x_1, \ldots, x_{n_t-1}), \quad (8.74)
\end{aligned}
$$

where the last equality is a consequence of the chain rule of mutual information (see (B.18) in Appendix B). Let us look at the kth term in the chain rule expansion: $I(x_k; \mathbf{y}|x_1, \ldots, x_{k-1})$. Conditional on $x_1, \ldots, x_{k-1}$, we can subtract their effect from the output and obtain

$$\mathbf{y}' := \mathbf{y} - \sum_{i=1}^{k-1} \mathbf{h}_i x_i = \mathbf{h}_k x_k + \sum_{i>k} \mathbf{h}_i x_i + \mathbf{w}.$$

Thus,

$$I(x_k; \mathbf{y}|x_1, \ldots, x_{k-1}) = I(x_k; \mathbf{y}') = I(x_k; \mathbf{v}_{\text{mmse}}^*\mathbf{y}'), \tag{8.75}$$

where $\mathbf{v}_{\text{mmse}}$ is the MMSE filter for estimating x_k from $\mathbf{y}'$ and the last equality follows directly from the fact that the MMSE receiver is information-lossless. Hence, the rate achieved in kth stage of the MMSE–SIC receiver is precisely $I(x_k; \mathbf{y}|x_1, \ldots, x_{k-1})$, and the total rate achieved by this receiver is precisely the overall mutual information between the input $\mathbf{x}$ and the output $\mathbf{y}$ of the MIMO channel.

We now see why the MMSE filter is special: its scalar output preserves the information in the received vector about x_k. This property does not hold for other filters such as the decorrelator or the matched filter.

In the special case of a MISO channel with a scalar output

$$y[m] = \sum_{k=1}^{n_t} h_k x_k[m] + w[m], \tag{8.76}$$

the MMSE receiver at the kth stage is reduced to simple scalar multiplication followed by decoding; thus it is equivalent to decoding x_k while treating signals from antennas $k+1, k+2, \ldots, n_t$ as Gaussian interference. If we interpret (8.76) as an uplink channel with n_t users, the MMSE–SIC receiver thus reduces to the SIC receiver introduced in Section 6.1. Here we see another explanation why the SIC receiver is optimal in the sense of achieving the sum rate $I(x_1, x_2, \ldots, x_K; y)$ of the K-user uplink channel: it "implements" the chain rule of mutual information.

Fading channel

Now consider communicating using the transceiver architecture in Figure 8.1 but with the MMSE–SIC receiver on a time-varying fading MIMO channel with receiver CSI. If $\mathbf{Q} = \mathbf{I}_{n_t}$, the MMSE–SIC receiver allows reliable communication at a sum of the rates of the data streams equal to the mutual information of the channel under inputs of the form

$$\mathcal{CN}(0, \mathrm{diag}\{P_1, \ldots, P_{n_t}\}). \tag{8.77}$$

In the case of i.i.d. Rayleigh fading, the optimal input is precisely $\mathcal{CN}(0, \mathbf{I}_{n_t})$, and so the MMSE–SIC receiver achieves the capacity as well.

More generally, we have seen that if a MIMO channel, viewed in the angular domain, can be modeled by a matrix $\mathbf{H}$ having zero mean, uncorrelated entries, then the optimal input distribution is always of the form in (8.77) (cf. Section 8.2.1 and Exercise 8.3). Independent data streams decoded using the MMSE–SIC receiver still achieve the capacity of such MIMO channels, but the data streams are now transmitted over the transmit angular windows (instead of directly on the antennas themselves). This means that the transceiver architecture of Figure 8.1 with $\mathbf{Q} = \mathbf{U}_t$ and the MMSE-SIC receiver, achieves the capacity of the fast fading MIMO channel.

Discussion 8.1 Connections with CDMA multiuser detection and ISI equalization

Consider the situation where independent data streams are sent out from each antenna (cf. (8.42)). Here the received vector is a combination of the streams arriving in different receive spatial signatures, with stream k having a receive spatial signature of $\mathbf{h}_k$. If we make the analogy between space and bandwidth, then (8.42) serves as a model for the uplink of a CDMA system: the streams are replaced by the users (since the users cannot cooperate, the independence between them is justified naturally) and $\mathbf{h}_k$ now represents the *received* signature sequence of user k. The number of receive antennas is replaced by

the number of chips in the CDMA signal. The base-station has access to the received signal and decodes the information simultaneously communicated by the different users. The base-station could use a bank of linear filters with or without successive cancellation. The study of the receiver design at the base-station, its complexities and performance, is called *multiuser detection*. The progress of multiuser detection is well chronicled in [131].

Another connection can be drawn to point-to-point communication over frequency-selective channels. In our study of the OFDM approach to communicating over frequency-selective channels in Section 3.4.4, we expressed the effect of the ISI in a matrix form (see (3.139)). This representation suggests the following interpretation: communicating over a block length of N_c on the L-tap time-invariant frequency-selective channel (see (3.129)) is equivalent to communicating over an $N_c \times N_c$ MIMO channel. The equivalent MIMO channel **H** is related to the taps of the frequency-selective channel, with the ℓth tap denoted by h_ℓ (for $\ell \geq L$, the tap $h_\ell = 0$), is

$$H_{ij} = \begin{cases} h_{i-j} & \text{for } i \geq j, \\ 0 & \text{otherwise.} \end{cases} \tag{8.78}$$

Due to the nature of the frequency-selective channel, previously transmitted symbols act as interference to the current symbol. The study of appropriate techniques to recover the transmit symbols in a frequency-selective channel is part of classical communication theory under the rubric of *equalization*. In our analogy, the transmitted symbols at different times in the frequency-selective channel correspond to the ones sent over the transmit antennas. Thus, there is a natural analogy between equalization for frequency-selective channels and transceiver design for MIMO channels (Table 8.1).

Table 8.1 Analogies between ISI equalization and MIMO communication techniques. We have covered all of these except the last one, which will be discussed in Chapter 10.

ISI equalization	MIMO communication
OFDM	SVD
Linear zero-forcing equalizer	Decorrelator/interference nuller
Linear MMSE equalizer	Linear MMSE receiver
Decision feedback equalizer (DFE)	Successive interference cancellation (SIC)
ISI precoding	Costa precoding

8.4 Slow fading MIMO channel

We now turn our attention to the slow fading MIMO channel,

$$\mathbf{y}[m] = \mathbf{H}\mathbf{x}[m] + \mathbf{w}[m], \tag{8.79}$$

where $\mathbf{H}$ is fixed over time but random. The receiver is aware of the channel realization but the transmitter only has access to its statistical characterization. As usual, there is a total transmit power constraint P. Suppose we want to communicate at a target rate R bits/s/Hz. If the transmitter were aware of the channel realization, then we could use the transceiver architecture in Figure 8.1 with an appropriate allocation of rates to the data streams to achieve reliable communication as long as

$$\log \det \left(\mathbf{I}_{n_{\mathrm{r}}} + \frac{1}{N_0} \mathbf{H}\mathbf{K}_x\mathbf{H}^* \right) > R, \tag{8.80}$$

where the total transmit power constraint implies a condition on the covariance matrix: $\mathrm{Tr}[\mathbf{K}_x] \leq P$. However, remarkably, information theory guarantees the existence of a *channel-state independent* coding scheme that achieves reliable communication whenever the condition in (8.80) is met. Such a code is *universal*, in the sense that it achieves reliable communication on every MIMO channel satisfying (8.80). This is similar to the universality of the code achieving the outage performance on the slow fading parallel channel (cf. Section 5.4.4). When the MIMO channel does not satisfy the condition in (8.80), then we are in outage. We can choose the transmit strategy (parameterized by the covariance) to minimize the probability of the outage event:

$$p_{\mathrm{out}}^{\mathrm{mimo}}(R) = \min_{\mathbf{K}_x:\mathrm{Tr}[\mathbf{K}_x]\leq P} \mathbb{P}\left\{ \log \det \left(\mathbf{I}_{n_{\mathrm{r}}} + \frac{1}{N_0} \mathbf{H}\mathbf{K}_x\mathbf{H}^* \right) < R \right\}. \tag{8.81}$$

Section 8.5 describes a transceiver architecture which achieves this outage performance.

The solution to this optimization problem depends, of course, on the statistics of channel $\mathbf{H}$. For example, if $\mathbf{H}$ is deterministic, the optimal solution is to perform a singular value decomposition of $\mathbf{H}$ and waterfill over the eigenmodes. When $\mathbf{H}$ is random, then one cannot tailor the covariance matrix to one particular channel realization but should instead seek a covariance matrix that works well statistically over the ensemble of the channel realizations.

It is instructive to compare the outage optimization problem (8.81) with that of computing the fast fading capacity with receiver CSI (cf. (8.10)). If we think of

$$f(\mathbf{K}_x, \mathbf{H}) := \log \det \left(\mathbf{I}_{n_{\mathrm{r}}} + \frac{1}{N_0} \mathbf{H}\mathbf{K}_x\mathbf{H}^* \right), \tag{8.82}$$

as the rate of information flow over the channel $\mathbf{H}$ when using a coding strategy parameterized by the covariance matrix $\mathbf{K}_x$, then the fast fading capacity is

$$C = \max_{\mathbf{K}_x : \mathrm{Tr}[\mathbf{K}_x] \leq P} \mathbb{E}_{\mathbf{H}}[f(\mathbf{K}_x, \mathbf{H})], \qquad (8.83)$$

while the outage probability is

$$p_{\mathrm{out}}(R) = \min_{\mathbf{K}_x : \mathrm{Tr}[\mathbf{K}_x] \leq P} \mathbb{P}\{f(\mathbf{K}_x, \mathbf{H}) < R\}. \qquad (8.84)$$

In the fast fading scenario, one codes over the fades through time and the relevant performance metric is the long-term average rate of information flow that is permissible through the channel. In the slow fading scenario, one is only provided with a single realization of the channel and the objective is to minimize the probability that the rate of information flow falls below the target rate. Thus, the former is concerned with maximizing the expected value of the random variable $f(\mathbf{K}_x, \mathbf{H})$ and the latter with minimizing the tail probability that the same random variable is less than the target rate. While maximizing the expected value typically helps to reduce this tail probability, in general there is no one-to-one correspondence between these two quantities: the tail probability depends on higher-order moments such as the variance.

We can consider the i.i.d. Rayleigh fading model to get more insight into the nature of the optimizing covariance matrix. The optimal covariance matrix over the fast fading i.i.d. Rayleigh MIMO channel is $\mathbf{K}_x^* = P/n_t \cdot \mathbf{I}_{n_t}$. This covariance matrix transmits isotropically (in all directions), and thus one would expect that it is also good in terms of reducing the variance of the information rate $f(\mathbf{K}_x, \mathbf{H})$ and, indirectly, the tail probability. Indeed, we have seen (cf. Section 5.4.3 and Exercise 5.16) that this is the optimal covariance in terms of outage performance for the MISO channel, i.e., $n_r = 1$, at high SNR. In general, [119] conjectures that this is the optimal covariance matrix for the i.i.d. Rayleigh slow fading MIMO channel at high SNR. Hence, the resulting outage probability

$$p_{\mathrm{out}}^{\mathrm{iid}}(R) = \mathbb{P}\left\{ \log \det\left(\mathbf{I}_{n_r} + \frac{\mathsf{SNR}}{n_t}\mathbf{H}\mathbf{H}^* \right) < R \right\}, \qquad (8.85)$$

is often taken as a good upper bound to the actual outage probability at high SNR.

More generally, the conjecture is that it is optimal to restrict to a subset of the antennas and then transmit isotropically among the antennas used. The number of antennas used depends on the SNR level: the lower the SNR level relative to the target rate, the smaller the number of antennas used. In particular, at very low SNR relative to the target rate, it is optimal to use just one transmit antenna. We have already seen the validity of this conjecture

in the context of a single receive antenna (cf. Section 5.4.3) and we are considering a natural extension to the MIMO situation. However, at typical outage probability levels, the SNR is high relative to the target rate and it is expected that using all the antennas is a good strategy.

High SNR

What outage performance can we expect at high SNR? First, we see that the MIMO channel provides increased diversity. We know that with $n_r = 1$ (the MISO channel) and i.i.d. Rayleigh fading, we get a diversity gain equal to n_t. On the other hand, we also know that with $n_t = 1$ (the SIMO channel) and i.i.d. Rayleigh fading, the diversity gain is equal to n_r. In the i.i.d. Rayleigh fading MIMO channel, we can achieve a diversity gain of $n_t \cdot n_r$, which is the number of independent random variables in the channel. A simple repetition scheme of using one transmit antenna at a time to send the same symbol x successively on the different n_t antennas over n_t consecutive symbol periods, yields an equivalent scalar channel

$$\tilde{y} = \sum_{i=1}^{n_r} \sum_{j=1}^{n_t} |h_{ij}|^2 x + w, \tag{8.86}$$

whose outage probability decays like $1/\mathsf{SNR}^{n_t n_r}$. Exercise 8.23 shows the unsurprising fact that the outage probability of the i.i.d. Rayleigh fading MIMO channel decays no faster than this.

Thus, a MIMO channel yields a diversity gain of exactly $n_t \cdot n_r$. The corresponding ϵ-outage capacity of the MIMO channel benefits from both the diversity gain and the spatial degrees of freedom. We will explore the high SNR characterization of the combined effect of these two gains in Chapter 9.

8.5 D-BLAST: an outage-optimal architecture

We have mentioned that information theory guarantees the existence of coding schemes (parameterized by the covariance matrix) that ensure reliable communication at rate R on every MIMO channel that satisfies the condition (8.80). In this section, we will derive a transceiver architecture that achieves the outage performance. We begin with considering the performance of the V-BLAST architecture in Figure 8.1 on the slow fading MIMO channel.

8.5.1 Suboptimality of V-BLAST

Consider the V-BLAST architecture in Figure 8.1 with the MMSE–SIC receiver structure (cf. Figure 8.16) that we have shown to achieve the

capacity of the *fast* fading MIMO channel. This architecture has two main features:

- Independently coded data streams are multiplexed in an appropriate coordinate system $\mathbf{Q}$ and transmitted over the antenna array. Stream k is allocated an appropriate power P_k and an appropriate rate R_k.
- A bank of linear MMSE receivers, in conjunction with successive cancellation, is used to demodulate the streams (the MMSE–SIC receiver).

The MMSE–SIC receiver demodulates the stream from transmit antenna 1 using an MMSE filter, decodes the data, subtracts its contribution from the stream, and proceeds to stream 2, and so on. Each stream is thought of as a layer.

Can this same architecture achieve the optimal outage performance in the *slow fading* channel? In general, the answer is no. To see this concretely, consider the i.i.d. Rayleigh fading model. Here the data streams are transmitted over separate antennas and it is easy to see that each stream has a diversity of *at most* n_r: if the channel gains from the kth transmit antenna to *all* the n_r receive antennas are in deep fade, then the data in the kth stream will be lost. On the other hand, the MIMO channel itself provides a diversity gain of $n_t \cdot n_r$. Thus, V-BLAST does not exploit the full diversity available in the channel and therefore cannot be outage-optimal. The basic problem is that there is no coding across the streams so that if the channel gains from one transmit antenna are bad, the corresponding stream will be decoded in error.

We have said that, under the i.i.d. Rayleigh fading model, the diversity of each stream in V-BLAST is *at most* n_r. The diversity would be *exactly* n_r if it were the only stream being transmitted; with simultaneous transmission of streams, the diversity could be even lower depending on the receiver. This can be seen most clearly if we replace the bank of linear MMSE receivers in V-BLAST with a bank of decorrelators and consider the case $n_t \leq n_r$. In this case, the distribution of the output SNR at each stage can be explicitly computed; this was actually done in Section 8.3.2:

$$\mathsf{SINR}_k \sim \frac{P_k}{N_0} \cdot \chi^2_{2[n_r - (n_t - k)]}. \tag{8.87}$$

The diversity of the kth stream is therefore $n_r - (n_t - k)$. Since $n_t - k$ is the number of uncancelled interfering streams at the kth stage, one can interpret this as saying that the loss of diversity due to interference is precisely the number of interferers needed to be nulled out. The first stream has the worst diversity of $n_r - n_t + 1$; this is also the bottleneck of the whole system because the correct decoding of subsequent streams depends on the correct decoding and cancellation of this stream. In the case of a square system, the first stream has a diversity of only 1, i.e., no diversity gain. We have already seen this result in the special case of the 2×2 example in Section 3.3.3. Though this

analysis is for the decorrelator, it turns out that the MMSE receiver yields exactly the same diversity gain (see Exercise 8.24). Using joint ML detection of the streams, on the other hand, a diversity of n_r can be recovered (as in the 2×2 example in Section 3.3.3). However, this is still far away from the full diversity gain $n_t n_r$ of the channel.

There are proposed improvements to the basic V-BLAST architecture. For instance, adapting the cancellation order as a function of the channel, and allocating different rates to different streams depending on their position in the cancellation order. However, none of these variations can provide a diversity larger than n_r, as long as we are sending independently coded streams on the transmit antennas.

A more careful look

Here is a more precise understanding of why V-BLAST is suboptimal, which will suggest how V-BLAST can be improved. For a given $\mathbf{H}$, (8.71) yields the following decomposition:

$$\log \det(\mathbf{I}_{n_r} + \mathbf{H}\mathbf{K}_x\mathbf{H}^*) = \sum_{k=1}^{n_t} \log(1 + \mathsf{SINR}_k). \tag{8.88}$$

SINR_k is the output signal-to-interference-plus-noise ratio of the MMSE demodulator at the kth stage of the cancellation. The output SINRs are random since they are a function of the channel matrix $\mathbf{H}$. Suppose we have a target rate of R and we split this into rates $R_1, \ldots, R_{n_t}$ allocated to the individual streams. Suppose that the transmit strategy (parameterized by the covariance matrix $\mathbf{K}_x := \mathbf{Q} \operatorname{diag}\{P_1, \ldots, P_{n_t}\}\mathbf{Q}^*$, cf. (8.3)) is chosen to be the one that yields the outage probability in (8.81). Now we note that the *channel* is in outage if

$$\log \det(\mathbf{I}_{n_r} + \mathbf{H}\mathbf{K}_x\mathbf{H}^*) < R, \tag{8.89}$$

or equivalently,

$$\sum_{k=1}^{n_t} \log(1 + \mathsf{SINR}_k) < \sum_{k=1}^{n_t} R_k. \tag{8.90}$$

However, V-BLAST is in outage as long as the random SINR in *any* stream cannot support the rate allocated to that stream, i.e.,

$$\log(1 + \mathsf{SINR}_k) < R_k, \tag{8.91}$$

for any k. Clearly, this can occur even when the channel is not in outage. Hence, V-BLAST cannot be universal and is not outage-optimal. This problem

did not appear in the fast fading channel because there we code over the temporal channel *variations* and thus kth stream gets a *deterministic* rate of

$$\mathbb{E}[\log(1 + \mathsf{SINR}_k)] \text{ bits/s/Hz.} \tag{8.92}$$

8.5.2 Coding across transmit antennas: D-BLAST

Significant improvement of V-BLAST has to come from coding *across* the transmit antennas. How do we improve the architecture to allow that? To see more clearly how to proceed, one can draw an analogy between V-BLAST and the *parallel fading channel*. In V-BLAST, the kth stream effectively sees a channel with a (random) signal-to-noise ratio SINR_k; this can therefore be viewed as a parallel channel with n_t sub-channels. In V-BLAST, there is no coding across these sub-channels: outage therefore occurs whenever one of these sub-channels is in a deep fade and cannot support the rate of the stream using that sub-channel. On the other hand, by coding across the sub-channels, we can average over the randomness of the individual sub-channels and get better outage performance. From our discussion on parallel channels in Section 5.4.4, we know reliable communication is possible whenever

$$\sum_{k=1}^{n_t} \log(1 + \mathsf{SINR}_k) > R. \tag{8.93}$$

Figure 8.18 How D-BLAST works. (a) A soft estimate of block *A* of the first codeword (layer) obtained without interference. (b) A soft MMSE estimate of block *B* is obtained by suppressing the interference from antenna 2. (c) The soft estimates are combined to decode the first codeword (layer). (d) The first codeword is cancelled and the process restarts with the second codeword (layer).

From the decomposition (8.88), we see that this is exactly the no-outage condition of the original MIMO channel as well. Therefore, it seems that universal codes for the parallel channel can be transformed directly into universal codes for the original MIMO channel.

However, there is a problem here. To obtain the second sub-channel (with SINR_2), we are assuming that the first stream is already decoded and its received signal is cancelled off. However, to code across the sub-channels, the two streams should be *jointly* decoded. There seems to be a chicken-and-egg problem: without decoding the first stream, one cannot cancel its signal and get the second stream in the first place. The key idea to solve this problem is to *stagger* multiple codewords so that each codeword spans multiple transmit antennas but the symbols sent simultaneously by the different transmit antennas belong to different codewords.

Let us go through a simple example with two transmit antennas (Figure 8.18). The ith codeword $\mathbf{x}^{(i)}$ is made up of two blocks, $\mathbf{x}_A^{(i)}$ and $\mathbf{x}_B^{(i)}$, each of length N. In the first N symbol times, the first antenna sends nothing. The second antenna sends $\mathbf{x}_A^{(1)}$, block A of the first codeword. The receiver performs maximal ratio combining of the signals at the receive antennas to estimate $\mathbf{x}_A^{(1)}$; this yields an equivalent sub-channel with signal-to-noise ratio SINR_2, since the other antenna is sending nothing.

In the second N symbol times, the first antenna sends $\mathbf{x}_B^{(1)}$ (block B of the first codeword), while the second antenna sends $\mathbf{x}_A^{(2)}$ (block A of the second

codeword). The receiver does a linear MMSE estimation of $\mathbf{x}_B^{(1)}$, treating $\mathbf{x}_A^{(2)}$ as interference to be suppressed. This produces an equivalent sub-channel of signal-to-noise ratio SINR_1. Thus, the first codeword as a whole now sees the parallel channel described above (Exercise 8.25), and, assuming the use of a universal parallel channel code, can be decoded provided that

$$\log(1 + \mathsf{SINR}_1) + \log(1 + \mathsf{SINR}_2) > R. \qquad (8.94)$$

Once codeword 1 is decoded, $\mathbf{x}_B^{(1)}$ can be subtracted off the received signal in the second N symbol times. This leaves $\mathbf{x}_A^{(2)}$ alone in the received signal, and the process can be repeated. Exercise 8.26 generalizes this architecture to arbitrary number of transmit antennas.

In V-BLAST, each coded stream, or layer, extends horizontally in the space-time grid and is placed vertically above another. In the improved architecture above, each layer is striped *diagonally* across the space-time grid (Figure 8.18). This architecture is naturally called Diagonal BLAST, or D-BLAST for short.

The D-BLAST scheme suffers from a rate loss because in the initialization phase some of the antennas have to be kept silent. For example, in the two transmit antenna architecture illustrated in Figure 8.18 (with $N = 1$ and 5 layers), two symbols are set to zero among the total of 10; this reduces the rate by a factor of 4/5 (Exercise 8.27 generalizes this calculation). So for a finite number of layers, D-BLAST does not achieve the outage performance of the MIMO channel. As the number of layers grows, the rate loss gets amortized and the MIMO outage performance is approached. In practice, D-BLAST suffers from *error propagation*: if one layer is decoded incorrectly, all subsequent layers are affected. This puts a practical limit on the number of layers which can be transmitted consecutively before re-initialization. In this case, the rate loss due to initialization and termination is not negligible.

8.5.3 Discussion

D-BLAST should really be viewed as a transceiver architecture rather than a space-time code: through signal processing and interleaving of the codewords across the antennas, it converts the MIMO channel into a parallel channel. As such, it allows the leveraging of any good parallel-channel code for the MIMO channel. In particular, a universal code for the parallel channel, when used in conjunction with D-BLAST, is a universal space-time code for the MIMO channel.

It is interesting to compare D-BLAST with the Alamouti scheme discussed in Chapters 3 and 5. The Alamouti scheme can also be considered as a transceiver architecture: it converts the 2×1 MISO slow fading channel into a SISO slow fading channel. Any universal code for the SISO channel when used in conjunction with the Alamouti scheme yields a universal code for the MISO channel. Compared to D-BLAST, the signal processing is

much simpler, and there are no rate loss or error propagation issues. On the other hand, D-BLAST works for an arbitrary number of transmit and receive antennas. As we have seen, the Alamouti scheme does not generalize to arbitrary numbers of transmit antennas (cf. Exercise 3.16). Further, we will see in Chapter 9 that the Alamouti scheme is strictly suboptimal in MIMO channels with multiple transmit *and* receive antennas. This is because, unlike D-BLAST, the Alamouti scheme does not exploit all the available degrees of freedom in the channel.

Chapter 8 The main plot

Capacity of fast fading MIMO channels
In a rich scattering environment with receiver CSI, the capacity is approximately

- $\min(n_t, n_r) \log \mathsf{SNR}$ at high SNR: a gain in spatial degrees of freedom;
- $n_r \mathsf{SNR} \log_2 e$ at low SNR: a receive beamforming gain.

With $n_t = n_r = n$, the capacity is approximately $nc^*(\mathsf{SNR})$ for all SNR. Here $c^*(\mathsf{SNR})$ is a constant.

Transceiver architectures

- **With full CSI** convert the MIMO channel into $n_{\min}$ parallel channels by an appropriate change in the basis of the transmit and receive signals. This transceiver structure is motivated by the *singular value decomposition* of any linear transformation: a composition of a rotation, a scaling operation, followed by another rotation.
- **With receiver CSI** send independent data streams over each of the transmit antennas. The ML receiver decodes the streams jointly and achieves capacity. This is called the V-BLAST architecture.

Reciever structures
- **Simple receiver structure** Decode the data streams *separately*. Three main structures:
  - *matched filter*: use the receive antenna array to beamform to the receive spatial signature of the stream. Performance close to capacity at low SNR.
  - *decorrelator*: project the received signal onto the subspace orthogonal to the receive spatial signatures of all the other streams.
    - to be able to do the projection operation, need $n_r \geq n_t$.
    - For $n_r \geq n_t$, the decorrelator bank captures all the spatial degrees of freedom at high SNR.
  - *MMSE*: linear receiver that optimally trades off capturing the energy of the data stream of interest and nulling the inter-stream interference. Close to optimal performance at both low and high SNR.

- **Successive cancellation** Decode the data streams sequentially, using the results of the decoding operation to cancel the effect of the decoded data streams on the received signal.

Bank of linear MMSE receivers with successive cancellation achieves the capacity of the fast fading MIMO channel at all SNR.

Outage performance of slow fading MIMO channels

The i.i.d. Rayleigh slow fading MIMO channel provides a diversity gain equal to the product of n_t and n_r. Since the V-BLAST architecture does not code across the transmit antennas, it can achieve a diversity gain of at most n_r. Staggered interleaving of the streams of V-BLAST among the transmit antennas achieves the full outage performance of the MIMO channel. This is the D-BLAST architecture.

8.6 Bibliographical notes

The interest in MIMO communications was sparked by the capacity analysis of Foschini [40], Foschini and Gans [41] and Telatar [119]. Foschini and Gans focused on analyzing the outage capacity of the slow fading MIMO channel, while Telatar studied the capacity of fixed MIMO channels under optimal waterfilling, ergodic capacity of fast fading channels under receiver CSI, as well as outage capacity of slow fading channels. The D-BLAST architecture was introduced by Foschini [40], while the V-BLAST architecture was considered by Wolniansky *et al.* [147] in the context of point-to-point MIMO communication.

The study of the linear receivers, decorrelator and MMSE, was initiated in the context of multiuser detection of CDMA signals. The research in multiuser detection is very well exposed and summarized in a book by Verdú [131], who was the pioneer in this field. In particular, decorrelators were introduced by Lupas and Verdú [77] and the MMSE receiver by Madhow and Honig [79]. The optimality of the MMSE receiver in conjunction with successive cancellation was shown by Varanasi and Guess [129].

The literature on random matrices as applied in communication theory is summarized by Tulino and Verdú [127]. The key result on the asymptotic distribution of the singular values of large random matrices used in this chapter is by Marčenko and Pastur [78].

8.7 Exercises

Exercise 8.1 (reciprocity) Show that the capacity of a time-invariant MIMO channel with n_t transmit, n_r receive antennas and channel matrix **H** is the same as that of the channel with n_r transmit, n_t receive antennas, matrix $\mathbf{H}^*$, and same total power constraint.

Exercise 8.2 Consider coding over a block of length N on the data streams in the transceiver architecture in Figure 8.1 to communicate over the time-invariant MIMO channel in (8.1).

1. Fix $\epsilon > 0$ and consider the ellipsoid $E^{(\epsilon)}$ defined as

$$\{\mathbf{a} : \mathbf{a}^* (\mathbf{H}\mathbf{K}_x\mathbf{H}^* \otimes \mathbf{I}_N + N_0\mathbf{I}_{n_rN})^{-1}\mathbf{a} \le N(n_r + \epsilon)\}. \tag{8.95}$$

Here we have denoted the tensor product (or Kronecker product) between matrices by the symbol $\otimes$. In particular, $\mathbf{H}\mathbf{K}_x\mathbf{H}^* \otimes \mathbf{I}_N$ is a $n_rN \times n_rN$ block diagonal matrix:

$$\mathbf{H}\mathbf{K}_x\mathbf{H}^* \otimes \mathbf{I}_N = \begin{bmatrix} \mathbf{H}\mathbf{K}_x\mathbf{H}^* & & & 0 \\ & \mathbf{H}\mathbf{K}_x\mathbf{H}^* & \\ & & \ddots & \\ 0 & & & \mathbf{H}\mathbf{K}_x\mathbf{H} \end{bmatrix}.$$

Show that, for every ϵ, the received vector $\mathbf{y}^N$ (of length n_rN) lies with high probability in the ellipsoid $E^{(\epsilon)}$, i.e.,

$$\mathbb{P}\{\mathbf{y}^N \in E^{(\epsilon)}\} \to 1, \quad \text{as } N \to \infty. \tag{8.96}$$

2. Show that the volume of the ellipsoid $E^{(0)}$ is equal to

$$\det(N_0\mathbf{I}_{n_r} + \mathbf{H}\mathbf{K}_x\mathbf{H}^*)^N \tag{8.97}$$

times the volume of a $2n_rN$-dimensional real sphere with radius $\sqrt{n_rN}$. This justifies the expression in (8.4).

3. Show that the noise vector $\mathbf{w}^N$ of length n_rN satisfies

$$\mathbb{P}\{\|\mathbf{w}^N\|^2 \le N_0N(n_r + \epsilon)\} \to 1, \quad \text{as } N \to \infty. \tag{8.98}$$

Thus $\mathbf{w}^N$ lives, with high probability, in a $2n_rN$-dimensional real sphere of radius $\sqrt{N_0n_rN}$. Compare the volume of this sphere to the volume of the ellipsoid in (8.97) to justify the expression in (8.5).

Exercise 8.3 [130, 126] Consider the angular representation $\mathbf{H}^a$ of the MIMO channel $\mathbf{H}$. We statistically model the entries of $\mathbf{H}^a$ as zero mean and jointly uncorrelated.

1. Starting with the expression in (8.10) for the capacity of the MIMO channel with receiver CSI and substituting $\mathbf{H} := \mathbf{U}_r\mathbf{H}^a\mathbf{U}_t^*$, show that

$$C = \max_{\mathbf{K}_x : Tr\mathbf{K}_x \le P} \mathbb{E}\left[\log \det\left(\mathbf{I}_{n_r} + \frac{1}{N_0}\mathbf{H}^a\mathbf{U}_t^*\mathbf{K}_x\mathbf{U}_t\mathbf{H}^{a*}\right)\right]. \tag{8.99}$$

2. Show that we can restrict the input covariance in (8.99), without changing the maximal value, to be of the following special structure:

$$\mathbf{K}_x = \mathbf{U}_t\mathbf{\Lambda}\mathbf{U}_t^*, \tag{8.100}$$

where $\mathbf{\Lambda}$ is a diagonal matrix with non-negative entries that sum to P. *Hint*: We can always consider a covariance matrix of the form

$$\mathbf{K}_x = \mathbf{U}_t \tilde{\mathbf{K}}_x \mathbf{U}_t^*, \tag{8.101}$$

with $\tilde{\mathbf{K}}$ also a covariance matrix satisfying the total power constraint. To show that $\tilde{\mathbf{K}}$ can be restricted to be diagonal, consider the following decomposition:

$$\tilde{\mathbf{K}}_x = \mathbf{\Lambda} + \mathbf{K}_{off}, \tag{8.102}$$

where $\mathbf{\Lambda}$ is a diagonal matrix and $\mathbf{K}_{off}$ has zero diagonal elements (and thus contains all the off-diagonal elements of $\tilde{\mathbf{K}}$). Validate the following sequence of inequalities:

$$\mathbb{E}\left[\log\det\left(\mathbf{I}_{n_r} + \frac{1}{N_0}\mathbf{H}^a\mathbf{K}_{off}\mathbf{H}^{a*}\right)\right] \leq \log\mathbb{E}\left[\det\left(\mathbf{I}_{n_r} + \frac{1}{N_0}\mathbf{H}^a\mathbf{K}_{off}\mathbf{H}^{a*}\right)\right], \tag{8.103}$$

$$= \log\det\left(\mathbb{E}\left[\mathbf{I}_{n_r} + \frac{1}{N_0}\mathbf{H}^a\mathbf{K}_{off}\mathbf{H}^{a*}\right]\right), \tag{8.104}$$

$$= 0. \tag{8.105}$$

You can use Jensen's inequality (cf. Exercise B.2) to get (8.103). In (8.104), we have denoted $\mathbb{E}[\mathbf{X}]$ to be the matrix with (i, j)th entry equal to $\mathbb{E}[\mathbf{X}_{ij}]$. Now use the property that the elements of $\mathbf{H}^a$ are uncorrelated in arriving at (8.104) and (8.105). Finally, using the decomposition in (8.102), conclude (8.100), i.e., it suffices to consider covariance matrices $\tilde{\mathbf{K}}_x$ in (8.101) to be diagonal.

Exercise 8.4 [119] Consider i.i.d. Rayleigh fading, i.e., the entries of $\mathbf{H}$ are i.i.d. $\mathcal{CN}(0, 1)$, and the capacity of the fast fading channel with only receiver CSI (cf. (8.10)).

1. For i.i.d. Rayleigh fading, show that the distribution of $\mathbf{H}$ and that of $\mathbf{HU}$ are identical for every unitary matrix $\mathbf{U}$. This is a generalization of the rotational invariance of an i.i.d. complex Gaussian vector (cf. (A.22) in Appendix A).
2. Show directly for i.i.d. Rayleigh fading that the input covariance $\mathbf{K}_x$ in (8.10) can be restricted to be diagonal (without resorting to Exercise 8.3(2)).
3. Show further that among the diagonal matrices, the optimal input covariance is $(P/n_t)\mathbf{I}_{n_t}$. *Hint*: Show that the map

$$(p_1, \ldots, p_K) \mapsto \mathbb{E}\left[\log\det\left(\mathbf{I}_{n_r} + \frac{1}{N_0}\mathbf{H}\,\text{diag}\{p_1, \ldots, p_{n_t}\}\mathbf{H}^*\right)\right] \tag{8.106}$$

is jointly concave. Further show that the map is *symmetric*, i.e., reordering the argument $p_1, \ldots, p_{n_t}$ does not change the value. Observe that a jointly concave, symmetric function is maximized, subject to a sum constraint, exactly when all the function arguments are the same and conclude the desired result.

Exercise 8.5 Consider the uplink of the cellular systems studied in Chapter 4: the narrowband system (GSM), the wideband CDMA system (IS-95), and the wideband OFDM system (Flash-OFDM).

1. Suppose that the base-station is equipped with an array of multiple receive antennas. Discuss the impact of the receive antenna array on the performance of the three systems discussed in Chapter 4. Which system benefits the most?

2. Now consider the MIMO uplink, i.e., the mobiles are also equipped with multiple (transmit) antennas. Discuss the impact on the performance of the three cellular systems. Which system benefits the most?

Exercise 8.6 In Exercise 8.3 we have seen that the optimal input covariance is of the form $\mathbf{K}_x = \mathbf{U}_t \mathbf{\Lambda} \mathbf{U}_t^*$ with $\mathbf{\Lambda}$ a diagonal matrix. In this exercise, we study the situations under which $\mathbf{\Lambda}$ is $(P/n_t)\mathbf{I}_{n_t}$, making the optimal input covariance also equal to $(P/n_t)\mathbf{I}_{n_t}$. (We have already seen one instance when this is true in Exercise 8.4: the i.i.d. Rayleigh fading scenario.) Intuitively, this should be true whenever there is *complete* symmetry among the transmit angular windows. This heuristic idea is made precise below.

1. The symmetry condition formally corresponds to the following assumption on the columns (there are n_t of them, one for each of the transmit angular windows) of the angular representation $\mathbf{H}^a = \mathbf{U}_t \mathbf{H} \mathbf{U}_r^*$: the n_t column vectors are independent and, further, the vectors are identically distributed. We do not specify the joint distribution of the entries within any of the columns other than requiring that they have zero mean. With this symmetry condition, show that the optimal input covariance is $(P/n_t)\mathbf{I}_{n_t}$.

2. Using the previous part, or directly, strengthen the result of Exercise 8.4 by showing that the optimal input covariance is $(P/n_t)\mathbf{I}_{n_t}$ whenever

$$\mathbf{H} := [\mathbf{h}_1 \ldots \mathbf{h}_{n_t}], \qquad\qquad (8.107)$$

where $\mathbf{h}_1, \ldots, \mathbf{h}_{n_t}$ are i.i.d. $\mathcal{CN}(0, \mathbf{K}_h)$ for some covariance matrix $\mathbf{K}_h$.

Exercise 8.7 In Section 8.2.2, we showed that with receiver CSI the capacity of the i.i.d. Rayleigh fading $n \times n$ MIMO channel grows linearly with n at all SNR. In this reading exercise, we consider other statistical channel models which also lead to a linear increase of the capacity with n.

1. The capacity of the MIMO channel with i.i.d. entries (not necessarily Rayleigh), grows linearly with n. This result is derived in [21].

2. In [21], the authors also consider a *correlated* channel model: the entries of the MIMO channel are jointly complex Gaussian (with invertible covariance matrix). The authors show that the capacity still increases linearly with the number of antennas.

3. In [75], the authors show a linear increase in capacity for a MIMO channel with the number of i.i.d. entries growing quadratically in n (i.e., the number of i.i.d. entries is proportional to n^2, with the rest of the entries equal to zero).

Exercise 8.8 Consider the *block fading* MIMO channel (an extension of the single antenna model in Exercise 5.28):

$$\mathbf{y}[m + nT_c] = \mathbf{H}[n]\mathbf{x}[m + nT_c] + \mathbf{w}[m + nT_c], \qquad m = 1, \ldots, T_c, n \geq 1, \quad (8.108)$$

where T_c is the coherence time of the channel (measured in terms of the number of samples). The channel variations across the blocks $\mathbf{H}[n]$ are i.i.d. Rayleigh. A pilot based communication scheme transmits known symbols for k time samples at the beginning of each coherence time interval: each known symbol is sent over a different

transmit antenna, with the other transmit antennas silent. At high SNR, the k pilot symbols allow the receiver to *partially* estimate the channel: over the nth block, k of the n_t columns of $\mathbf{H}[n]$ are estimated with a high degree of accuracy. This allows us to reliably communicate on the $k \times n_r$ MIMO channel *with* receiver CSI.

1. Argue that the rate of reliable communication using this scheme at high SNR is approximately at least

$$\left(\frac{T_c - k}{T_c}\right) \min(k, n_r) \log \mathsf{SNR} \text{ bits/s/Hz}. \tag{8.109}$$

   Hint: An information theory fact says that replacing the effect of channel uncertainty as Gaussian noise (with the same covariance) can only make the reliable communication rate smaller.

2. Show that the optimal training time (and the corresponding number of transmit antennas to use) is

$$k^* := \min\left(n_t, n_r, \frac{T_c}{2}\right). \tag{8.110}$$

   Substituting this in (8.109) we see that the number of spatial degrees of freedom using the pilot scheme is equal to

$$\left(\frac{T_c - k^*}{T_c}\right) k^*. \tag{8.111}$$

3. A reading exercise is to study [155], which shows that the *capacity* of the non-coherent block fading channel at high SNR also has the same number of spatial degrees freedom as in (8.111).

Exercise 8.9 Consider the time-invariant frequency-selective MIMO channel:

$$\mathbf{y}[m] = \sum_{\ell=0}^{L-1} \mathbf{H}_\ell \mathbf{x}[m - \ell] + \mathbf{w}[m]. \tag{8.112}$$

Construct an appropriate OFDM transmission and reception scheme to transform the original channel to the following *parallel* MIMO channel:

$$\tilde{\mathbf{y}}_n = \tilde{\mathbf{H}}_n \tilde{\mathbf{x}}_n + \tilde{\mathbf{w}}_n, \qquad n = 0, \ldots, N_c - 1. \tag{8.113}$$

Here N_c is the number of OFDM tones. Identify $\tilde{\mathbf{H}}_n$, $n = 0, \ldots, N_c - 1$ in terms of $\mathbf{H}_\ell$, $\ell = 0, \ldots, L - 1$.

Exercise 8.10 Consider a fixed physical environment and a corresponding flat fading MIMO channel. Now suppose we double the transmit power constraint and the bandwidth. Argue that the capacity of the MIMO channel with receiver CSI exactly doubles. This scaling is consistent with that in the single antenna AWGN channel.

Exercise 8.11 Consider (8.42) where independent data streams $\{x_i[m]\}$ are transmitted on the transmit antennas ($i = 1 \ldots, n_t$):

$$\mathbf{y}[m] = \sum_{i=1}^{n_t} \mathbf{h}_i x_i[m] + \mathbf{w}[m]. \tag{8.114}$$

Assume $n_t \leq n_r$.

1. We would like to study the operation of the decorrelator in some detail here. So we make the assumption that $\mathbf{h}_i$ is not a linear combination of the other vectors $\mathbf{h}_1, \ldots, \mathbf{h}_{i-1}, \mathbf{h}_{i+1}, \ldots, \mathbf{h}_{n_t}$ for every $i = 1, \ldots, n_t$. Denoting $\mathbf{H} = [\mathbf{h}_1 \cdots \mathbf{h}_{n_t}]$, show that this assumption is equivalent to the fact that $\mathbf{H}^*\mathbf{H}$ is invertible.

2. Consider the following operation on the received vector in (8.114):

$$\hat{\mathbf{x}}[m] := (\mathbf{H}^*\mathbf{H})^{-1}\mathbf{H}^*\mathbf{y}[m] \tag{8.115}$$

$$= \mathbf{x}[m] + (\mathbf{H}^*\mathbf{H})^{-1}\mathbf{H}^*\mathbf{w}[m]. \tag{8.116}$$

Thus $\hat{x}_i[m] = x_i[m] + \tilde{w}_i[m]$ where $\tilde{\mathbf{w}}[m] := (\mathbf{H}^*\mathbf{H})^{-1}\mathbf{H}^*\mathbf{w}[m]$ is colored Gaussian noise. This means that the ith data stream sees no interference from any of the other streams in the received signal $\hat{x}_i[m]$. Show that $\hat{x}_i[m]$ must be the output of the decorrelator (up to a scaling constant) for the ith data stream and hence conclude the validity of (8.47). This property, and many more, about the decorrelator can be learnt from Chapter 5 of [99]. The special case of $n_t = n_r = 2$ can be verified by explicit calculations.

Exercise 8.12 Suppose $\mathbf{H}$ (with $n_t < n_r$) has i.i.d. $\mathcal{CN}(0, 1)$ entries and denote $\mathbf{h}_1, \ldots, \mathbf{h}_{n_t}$ as the columns of $\mathbf{H}$. Show that the probability that the columns are linearly dependent is zero. Hence, conclude that the probability that the rank of $\mathbf{H}$ is strictly smaller than n_t is zero.

Exercise 8.13 Suppose $\mathbf{H}$ (with $n_t < n_r$) has i.i.d. $\mathcal{CN}(0, 1)$ entries and denote the columns of $\mathbf{H}$ as $\mathbf{h}_1, \ldots, \mathbf{h}_{n_t}$. Use the result of Exercise 8.12 to show that the dimension of the subspace spanned by the vectors $\mathbf{h}_1, \ldots, \mathbf{h}_{k-1}, \mathbf{h}_{k+1}, \ldots, \mathbf{h}_{n_t}$ is $n_t - 1$ with probability 1. Hence conclude that the dimension of the subspace V_k, orthogonal to this one, has dimension $n_r - n_t + 1$ with probability 1.

Exercise 8.14 Consider the Rayleigh fading $n \times n$ MIMO channel $\mathbf{H}$ with i.i.d. $\mathcal{CN}(0, 1)$ entries. In the text we have discussed a random matrix result about the convergence of the empirical distribution of the singular values of $\mathbf{H}/\sqrt{n}$. It turns out that the condition number of $\mathbf{H}/\sqrt{n}$ converges to a deterministic limiting distribution. This means that the random matrix $\mathbf{H}$ is well-conditioned. The corresponding limiting density is given by

$$f(x) := \frac{4}{x^3}\, e^{-2/x^2}. \tag{8.117}$$

A reading exercise is to study the derivation of this result proved in Theorem 7.2 of [32].

Exercise 8.15 Consider communicating over the time-invariant $n_t \times n_r$ MIMO channel:

$$\mathbf{y}[m] = \mathbf{H}\mathbf{x}[m] + \mathbf{w}[m]. \tag{8.118}$$

The information bits are encoded using, say, a capacity-achieving Gaussian code such as an LDPC code. The encoded bits are then modulated into the transmit signal $\mathbf{x}[m]$; typically the components of the transmit vector belong to a regular constellation such as QAM. The receiver, typically, operates in two stages. The first stage is demodulation: at each time, soft information (a posteriori probabilities of the bits that modulated the

transmit vector) about the transmitted QAM symbol is evaluated. In the second stage, the soft information about the bits is fed to a channel decoder.

In this reading exercise, we study the first stage of the receiver. At time m, the demodulation problem is to find the QAM points composing the vector $\mathbf{x}[m]$ such that $\|\mathbf{y}[m] - \mathbf{H}\mathbf{x}[m]\|^2$ is the smallest possible. This problem is one of classical "least squares", but with the domain restricted to a finite set of points. When the modulation is QAM, the domain is a finite subset of the integer lattice. Integer least squares is known to be a computationally hard problem and several heuristic solutions, with less complexity, have been proposed. One among them is the *sphere decoding* algorithm. A reading exercise is to use [133] to understand the algorithm and an analysis of the average (over the fading channel) complexity of decoding.

Exercise 8.16 In Section 8.2.2 we showed two facts for the i.i.d. Rayleigh fading channel: (i) for fixed n and at low SNR, the capacity of a 1 by n channel approaches that of an n by n channel; (ii) for fixed SNR but large n, the capacity of a 1 by n channel grows only logarithmically with n while that of an n by n channel grows linearly with n. Resolve the apparent paradox.

Exercise 8.17 Verify (8.26). This result is derived in [132].

Exercise 8.18 Consider the channel (8.58):

$$\mathbf{y} = \mathbf{h}x + \mathbf{z}, \tag{8.119}$$

where $\mathbf{z}$ is $\mathcal{CN}(0, \mathbf{K}_z)$, $\mathbf{h}$ is a (complex) deterministic vector and x is the zero mean unknown (complex) random variable to be estimated. The noise $\mathbf{z}$ and the data symbol x are assumed to be uncorrelated.

1. Consider the following estimate of x from $\mathbf{y}$ using the vector $\mathbf{c}$ (normalized so that $\|\mathbf{c}\| = 1$):

$$\hat{x} := a\mathbf{c}^*\mathbf{y} = a\mathbf{c}^*\mathbf{h}x + a\mathbf{c}^*\mathbf{z}. \tag{8.120}$$

   Show that the constant a that minimizes the mean square error ($\mathbb{E}[|x - \hat{x}|^2]$) is equal to

$$\frac{\mathbb{E}[|x|^2]|\mathbf{c}^*\mathbf{h}|^2}{\mathbb{E}[|x|^2]|\mathbf{c}^*\mathbf{h}|^2 + \mathbf{c}^*\mathbf{K}_z\mathbf{c}} \frac{\mathbf{h}^*\mathbf{c}}{|\mathbf{h}^*\mathbf{c}|}. \tag{8.121}$$

2. Calculate the minimal mean square error (denoted by MMSE) of the linear estimate in (8.120) (by using the value of a in (8.121)). Show that

$$\frac{\mathbb{E}[|x|^2]}{\text{MMSE}} = 1 + \text{SNR} := 1 + \frac{\mathbb{E}[|x|^2]|\mathbf{c}^*\mathbf{h}|^2}{\mathbf{c}^*\mathbf{K}_z\mathbf{c}}. \tag{8.122}$$

3. Since we have shown that $\mathbf{c} = \mathbf{K}_z^{-1}\mathbf{h}$ maximizes the SNR (cf. (8.61)) among all linear estimators, conclude that this linear estimate (along with an appropriate choice of the scaling a, as in (8.121)), minimizes the mean square error in the linear estimation of x from (8.119).

Exercise 8.19 Consider detection on the generic vector channel with additive colored Gaussian noise (cf. (8.72)).

1. Show that the output of the linear MMSE receiver,

$$\mathbf{v}^*_{\text{mmse}}\mathbf{y}, \tag{8.123}$$

is a sufficient statistic to detect x from $\mathbf{y}$. This is a generalization of the scalar sufficient statistic extracted from the vector detection problem in Appendix A (cf. (A.55)).

2. From the previous part, we know that the random variables $\mathbf{y}$ and x are independent conditioned on $\mathbf{v}^*_{\text{mmse}}\mathbf{y}$. Use this to verify (8.73).

Exercise 8.20 We have seen in Figure 8.13 that, at low SNR, the bank of linear matched filter achieves capacity of the 8 by 8 i.i.d. Rayleigh fading channel, in the sense that the ratio of the total achievable rate to the capacity approaches 1. Show that this is true for general n_t and n_r.

Exercise 8.21 Consider the n by n i.i.d. flat Rayleigh fading channel. Show that the total achievable rate of the following receiver architectures scales linearly with n: (a) bank of linear decorrelators; (b) bank of matched filters; (c) bank of linear MMSE receivers. You can assume that independent information streams are coded and sent out of each of the transmit antennas and the power allocation across antennas is uniform. *Hint*: The calculation involving the linear MMSE receivers is tricky. You have to show that the linear MMSE receiver performance, asymptotically for large n, depends on the covariance matrix of the interference faced by each stream only through its empirical eigenvalue distribution, and then apply the large-n random matrix result used in Section 8.2.2. To show the first step, compute the mean and variance of the output SINR, conditional on the spatial signatures of the interfering streams. This calculation is done in [132, 123]

Exercise 8.22 Verify (8.71) by direct matrix manipulations.
Hint: You might find useful the following matrix inversion lemma (for invertible $\mathbf{A}$),

$$(\mathbf{A} + \mathbf{x}\mathbf{x}^*)^{-1} = \mathbf{A}^{-1} - \frac{\mathbf{A}^{-1}\mathbf{x}\mathbf{x}^*\mathbf{A}^{-1}}{1 + \mathbf{x}^*\mathbf{A}^{-1}\mathbf{x}}. \tag{8.124}$$

Exercise 8.23 Consider the outage probability of an i.i.d. Rayleigh MIMO channel (cf. (8.81)). Show that its decay rate in SNR (equal to P/N_0) is no faster than $n_t \cdot n_r$ by justifying each of the following steps.

$$p_{\text{out}}(R) \geq \mathbb{P}\{\log\det(\mathbf{I}_{n_r} + \mathsf{SNR}\,\mathbf{H}\mathbf{H}^*) < R\} \tag{8.125}$$

$$\geq \mathbb{P}\{\mathsf{SNR}\,\mathrm{Tr}[\mathbf{H}\mathbf{H}^*] < R\} \tag{8.126}$$

$$\geq (\mathbb{P}\{\mathsf{SNR}\,|h_{11}|^2 < R\})^{n_t n_r} \tag{8.127}$$

$$= \left(1 - e^{-\frac{R}{\mathsf{SNR}}}\right)^{n_t n_r} \tag{8.128}$$

$$\approx \frac{R^{n_t n_r}}{\mathsf{SNR}^{n_t n_r}}. \tag{8.129}$$

Exercise 8.24 Calculate the maximum diversity gains for each of the streams in the V-BLAST architecture using the MMSE–SIC receiver. *Hint*: At high SNR, interference seen by each stream is very high and the SINR of the linear MMSE receiver is very close to that of the decorrelator in this regime.

Exercise 8.25 Consider communicating over a 2×2 MIMO channel using the D-BLAST architecture with $N = 1$ and equal power allocation $P_1 = P_2 = P$ for both the layers. In this exercise, we will derive some properties of the parallel channel (with $L = 2$ diversity branches) created by the MMSE–SIC operation. We denote the MIMO channel by $\mathbf{H} = [\mathbf{h}_1, \mathbf{h}_2]$ and the projections

$$\mathbf{h}_{1\|2} := \frac{\mathbf{h}_1^* \mathbf{h}_2}{\|\mathbf{h}_2\|^2} \mathbf{h}_2, \qquad \mathbf{h}_{1\perp 2} := \mathbf{h}_1 - \mathbf{h}_{1\|2}. \tag{8.130}$$

Let us denote the induced parallel channel as

$$y_\ell = g_\ell x_\ell + w_\ell, \qquad \ell = 1, 2. \tag{8.131}$$

1. Show that

$$|g_1|^2 = \|\mathbf{h}_{1\perp 2}\|^2 + \frac{\|\mathbf{h}_{1\|2}\|^2}{\mathsf{SNR}\|\mathbf{h}_2\|^2 + 1}, \qquad |g_2|^2 = \|\mathbf{h}_2\|^2, \tag{8.132}$$

   where $\mathsf{SNR} = P/N_0$.
2. What is the marginal distribution of $|g_1|^2$ at high SNR? Are $|g_1|^2$ and $|g_2|^2$ positively correlated or negatively correlated?
3. What is the maximum diversity gain offered by this parallel channel?
4. Now suppose $|g_1|^2$ and $|g_2|^2$ in the parallel channel in (8.131) are independent, while still having the same marginal distribution as before. What is the maximum diversity gain offered by this parallel channel?

Exercise 8.26 Generalize the staggered stream structure (discussed in the context of a $2 \times n_r$ MIMO channel in Section 8.5) of the D-BLAST architecture to a MIMO channel with $n_t > 2$ transmit antennas.

Exercise 8.27 Consider a block length N D-BLAST architecture on a MIMO channel with n_t transmit antennas. Determine the rate loss due to the initialization phase as a function of N and n_t.